

Structure of the nutrient-sensing hub GATOR2

Max L. Valenstein^{1,2,8,*}, Kacper B. Rogala^{1,3,5,6,7,8,*}, Pranav V. Lalgudi^{1,2}, Edward J. Brignole^{2,4}, Xin Gu^{1,2}, Robert A. Saxton^{1,2}, Lynne Chantranupong^{1,2}, Jonas Kolibius¹, Jan-Philipp Quast¹, David M. Sabatini

¹Whitehead Institute for Biomedical Research, Cambridge, MA, USA.

²Department of Biology, Massachusetts Institute of Technology, Cambridge, MA, USA.

³Broad Institute of Harvard and Massachusetts Institute of Technology, Cambridge, MA, USA.

⁴MIT.nano, Massachusetts Institute of Technology, Cambridge, MA, USA.

⁵Stanford Cancer Institute, Stanford University School of Medicine, Stanford, CA, USA.

⁶Department of Structural Biology, Stanford University School of Medicine, Stanford, CA, USA.

⁷Department of Chemical and Systems Biology, Stanford University School of Medicine, Stanford, CA, USA.

⁸These authors contributed equally to this work.

*Correspondence: mvalenst@wi.mit.edu, rogala@stanford.edu

TABLE OF CONTENTS

Supplementary Figures

	Page
Supplementary Figure 1. Gel source images.	2
Supplementary Figure 2. Cryo-EM data collection and processing workflow.	30
Supplementary Figure 3. Structural determination of GATOR2.	31
Supplementary Figure 4. Generation of a composite GATOR2 map.	32
Supplementary Figure 5. Sequence alignment of MIOS.	33
Supplementary Figure 6. Sequence alignment of WDR24.	34
Supplementary Figure 7. Sequence alignment of WDR59.	35
Supplementary Figure 8. Sequence alignment of SEH1L.	36
Supplementary Figure 9. Sequence alignment of SEC13.	37

Supplementary Tables

Supplementary Table 1. Summary of cryo-EM data collection, 3D reconstruction, and model refinement.	38
---	----

Supplementary Figure 1 | part 1

Fig. 1b - Coomassie Stain

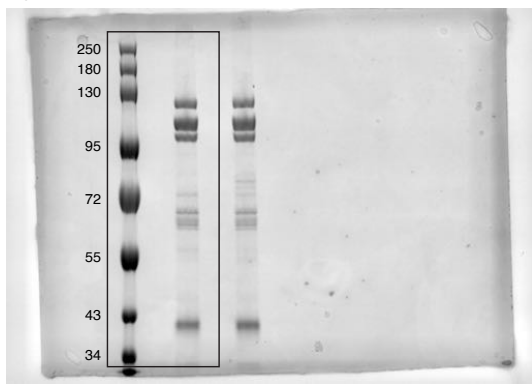


Fig. 1e - S6K pT389

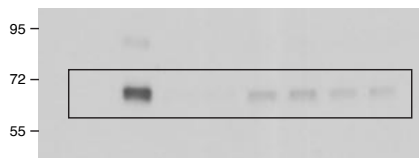


Fig. 1e - S6K

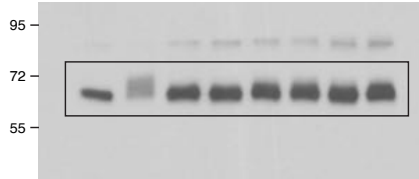


Fig. 1e - WDR24

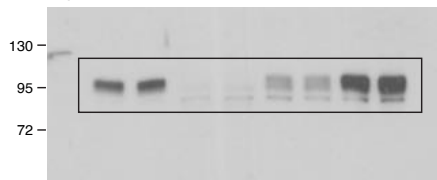


Fig. 1e - MIOS

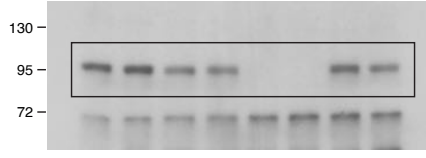


Fig. 1e - WDR59

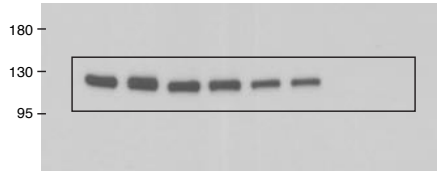


Fig. 1e - Raptor

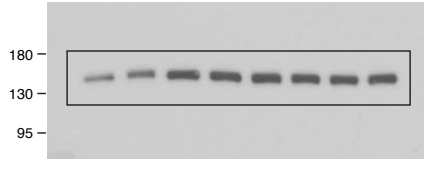


Fig. 2d - HA (IP)



Fig. 2d - FLAG-METAP2 (IP)



Fig. 2d - FLAG-MIOS-CTD (IP)



Fig. 2d - HA (cell lysate)

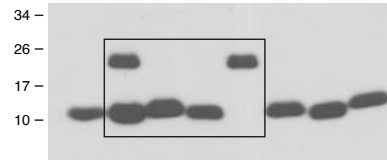


Fig. 2d - FLAG-METAP2 (cell lysate)

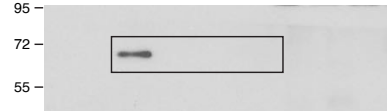
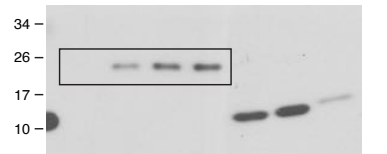


Fig. 2d - FLAG-MIOS-CTD (cell lysate)



Supplementary Fig. 1| Gel source images. Gel source images for Western blots and other SDS-PAGE based analyses.

Supplementary Figure 1 | part 2

Fig. 4a - CASTOR1-HA (IP)

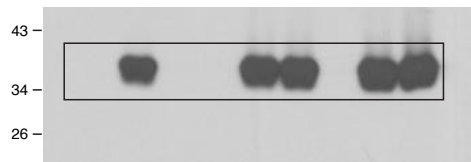


Fig. 4a - DEPDC5 (IP); short exposure

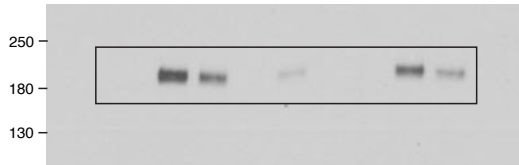


Fig. 4a - DEPDC5 (IP); long exposure

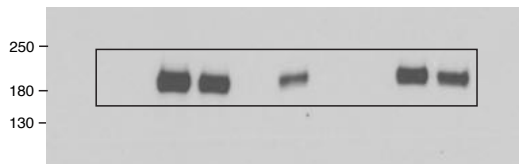


Fig. 4a - KPTN (IP)

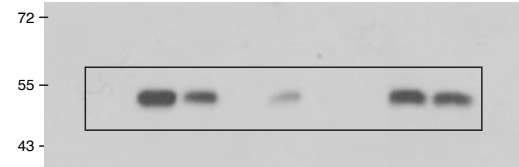


Fig. 4a - HA-Sestrin2 (IP)

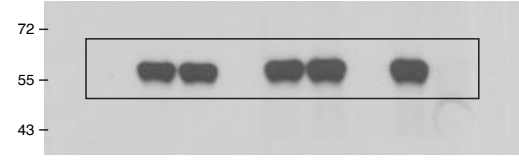


Fig. 4a - FLAG (IP)

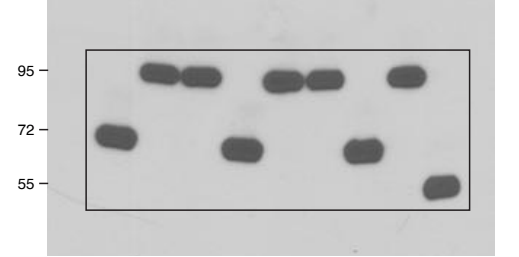


Fig. 4a - CASTOR1-HA (cell lysate)

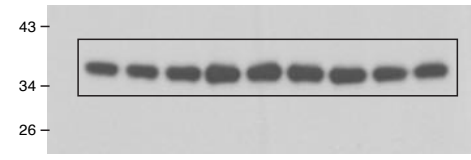


Fig. 4a - DEPDC5 (cell lysate)

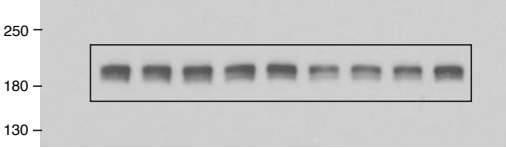


Fig. 4a - KPTN (cell lysate)

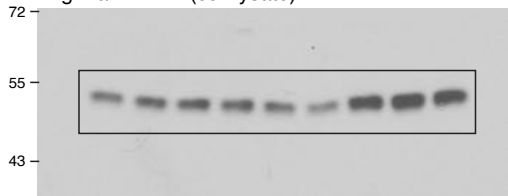


Fig. 4a - HA-Sestrin2 (cell lysate)

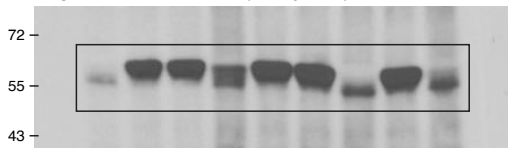


Fig. 4a - FLAG (cell lysate)

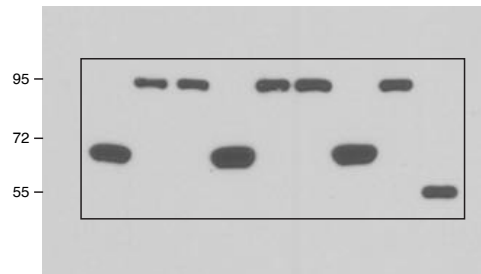


Fig. 4c - CASTOR1-HA (IP)



Fig. 4c - DEPDC5 (IP)



Fig. 4c - HA-Sestrin2 (IP)

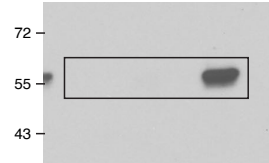
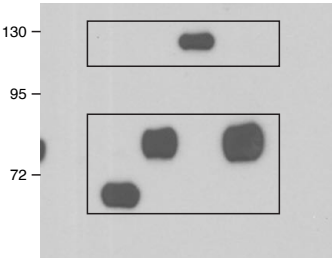
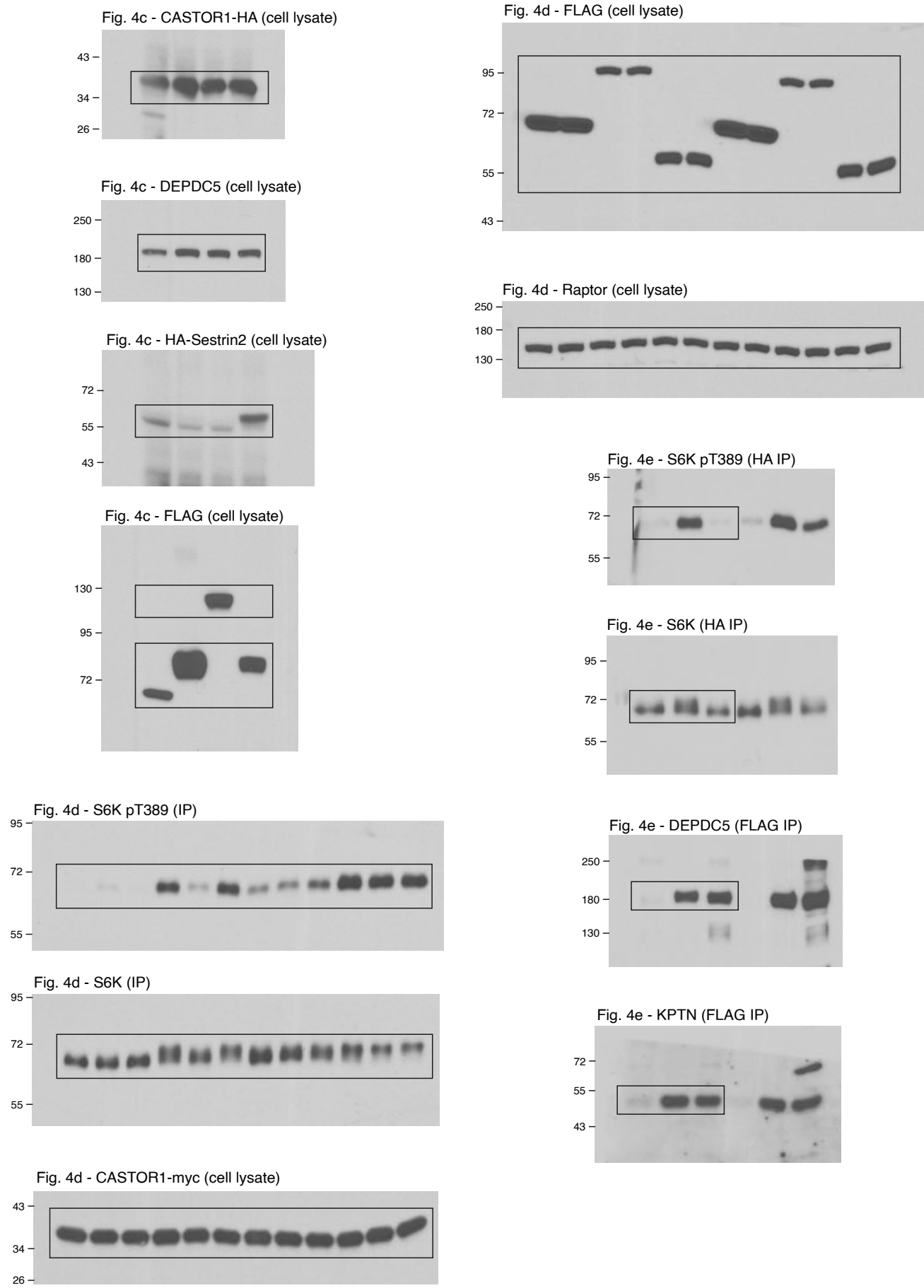


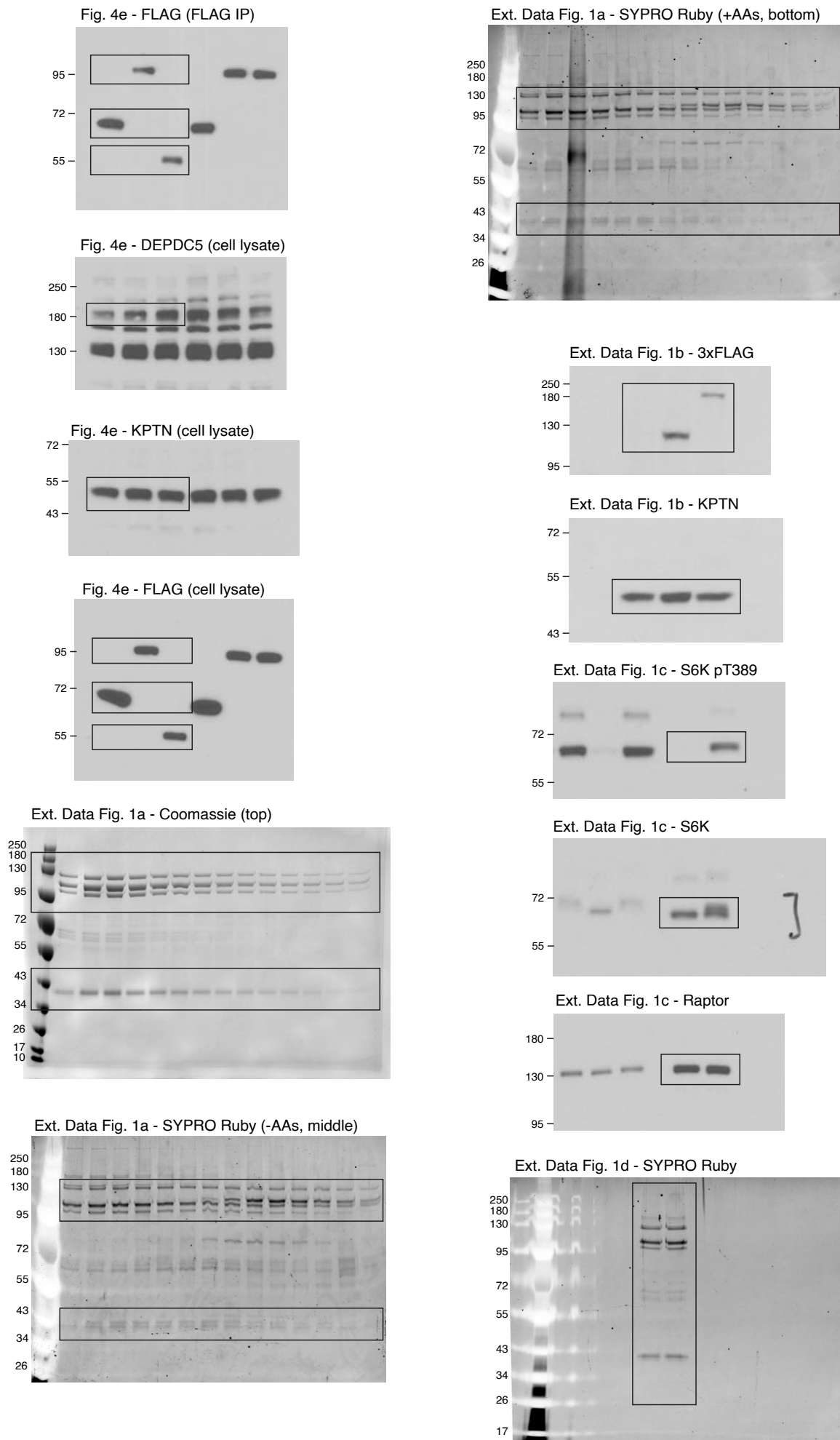
Fig. 4c - FLAG (IP)



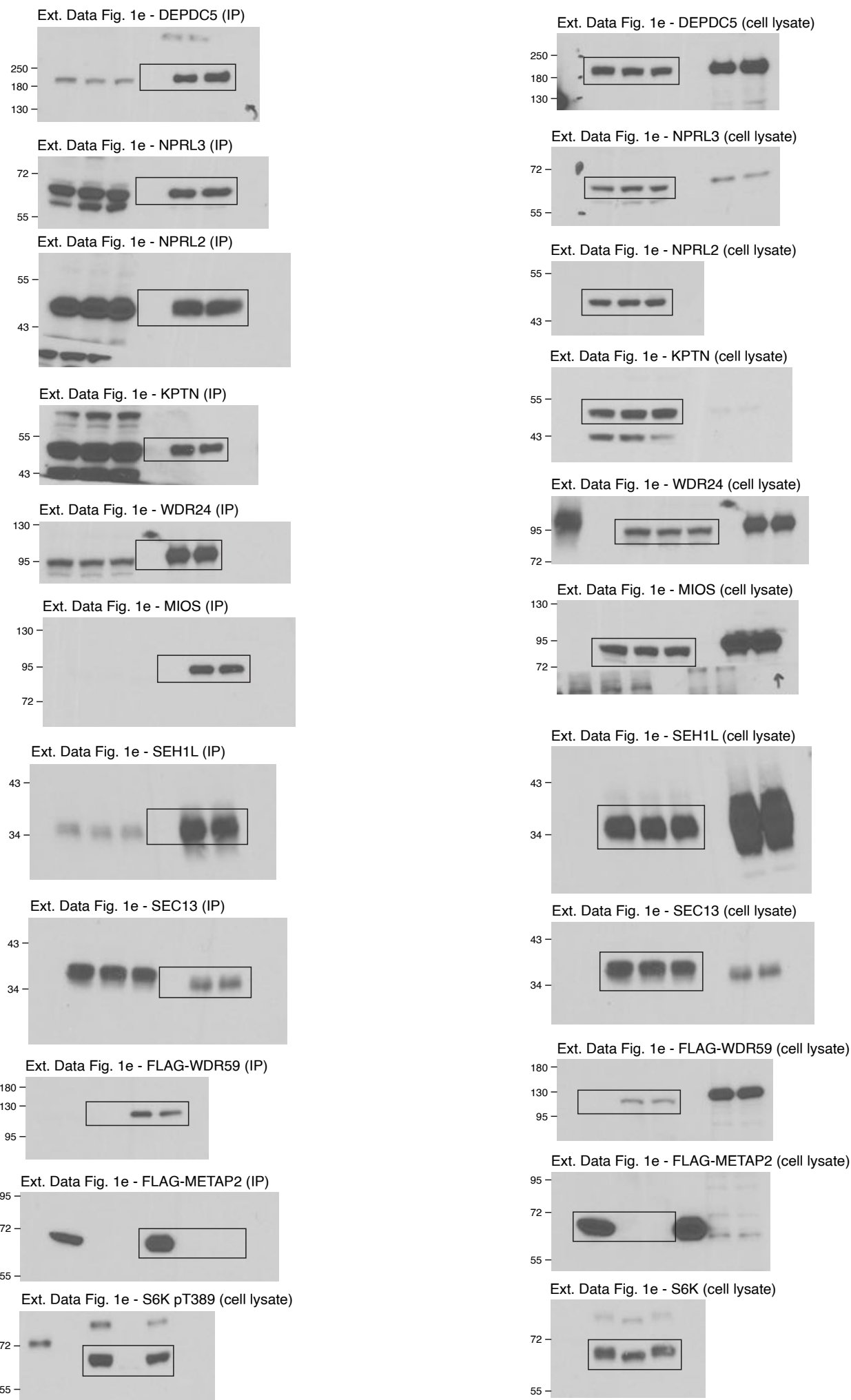
Supplementary Figure 1 | part 3



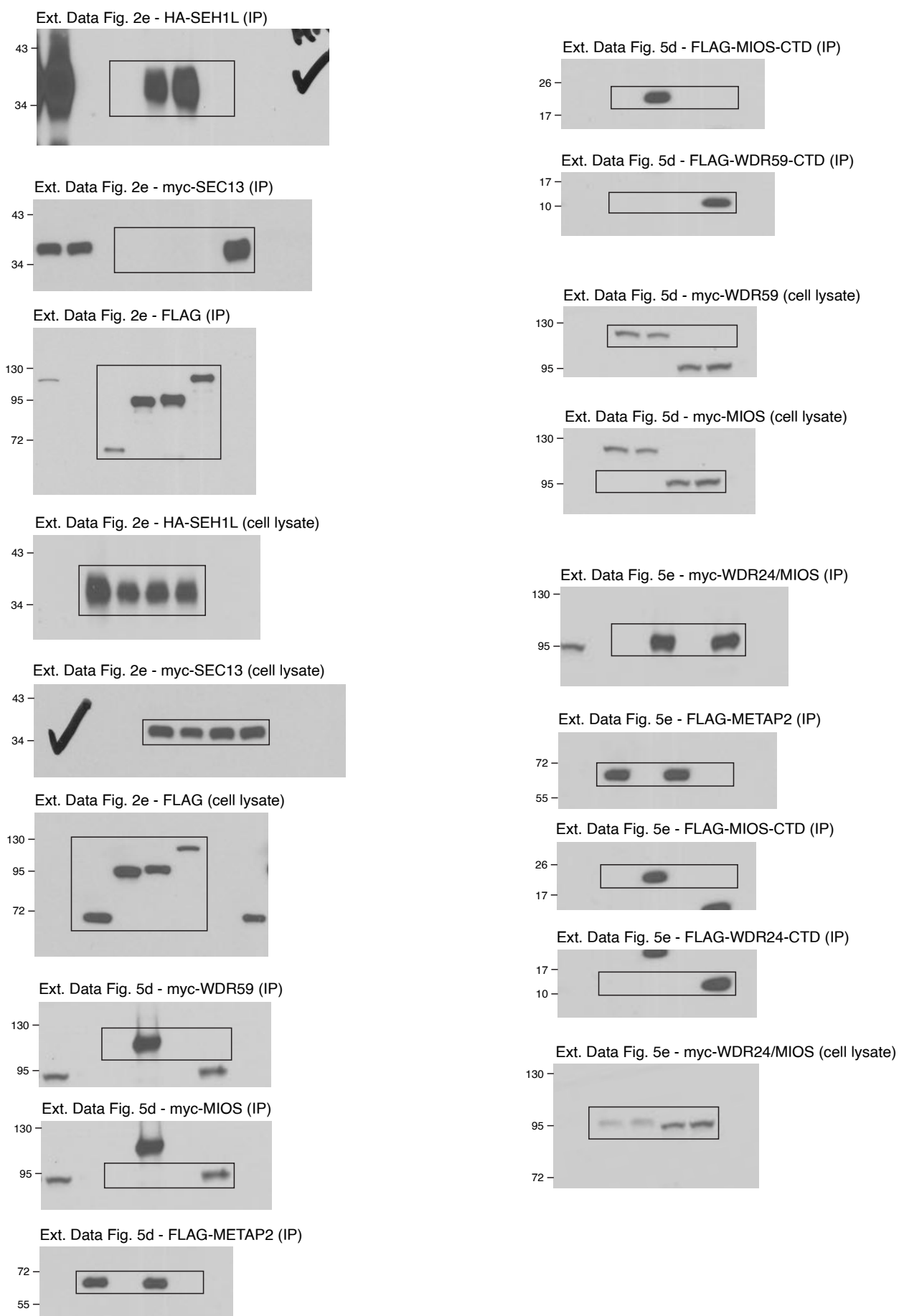
Supplementary Figure 1 | part 4



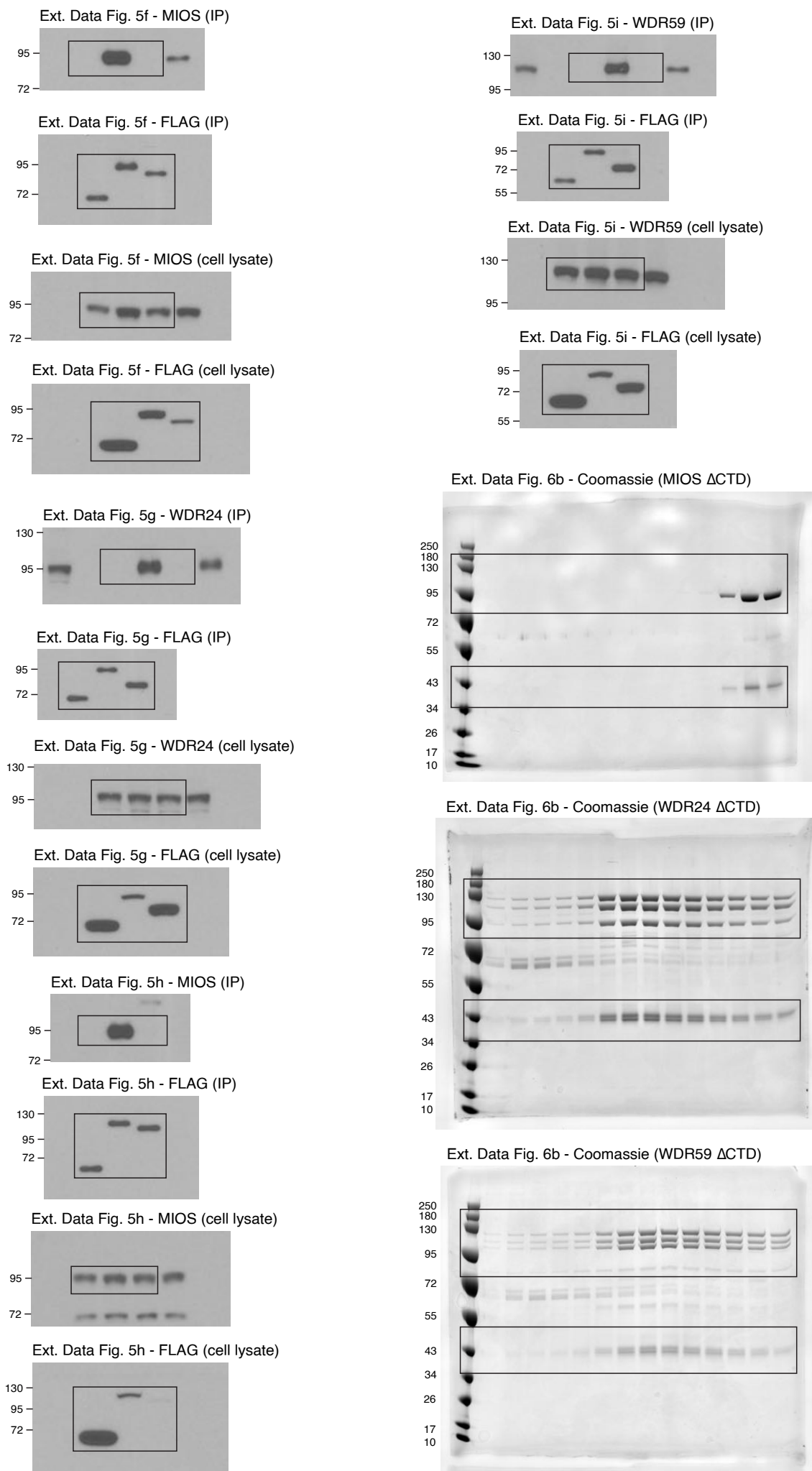
Supplementary Figure 1 | part 5



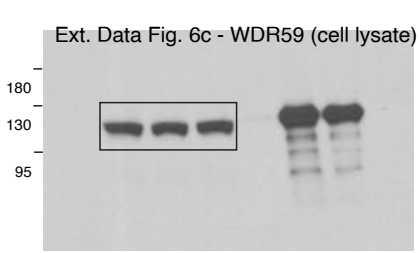
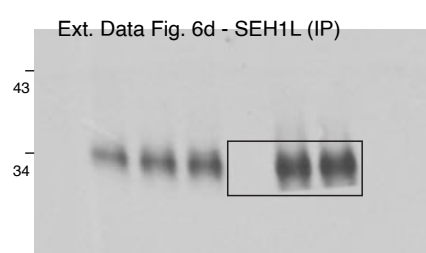
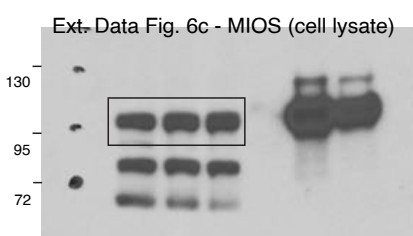
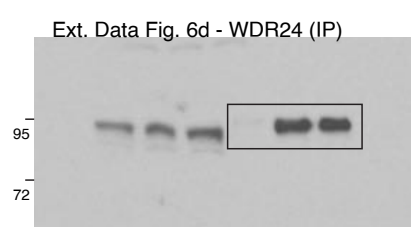
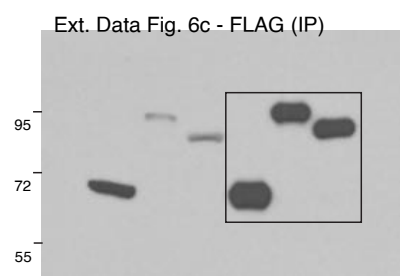
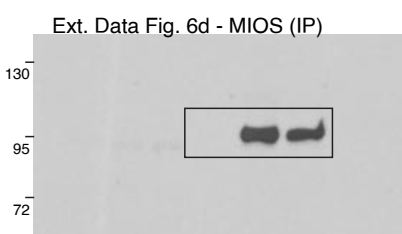
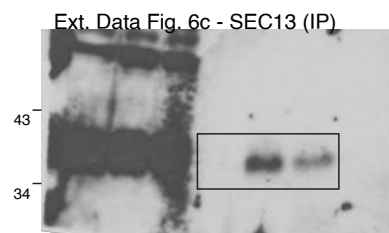
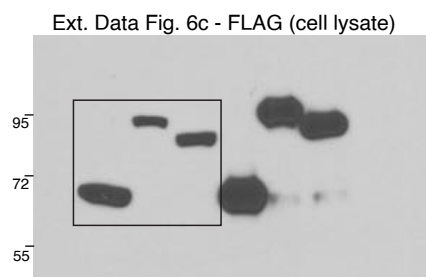
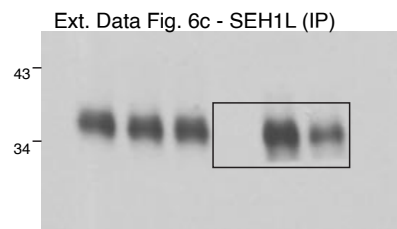
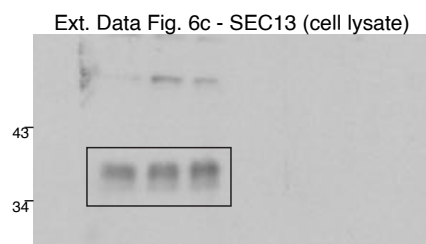
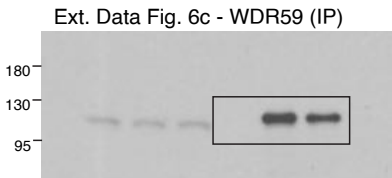
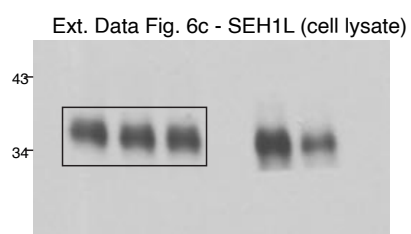
Supplementary Figure 1 | part 6



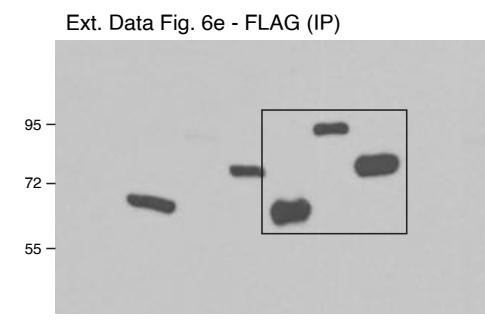
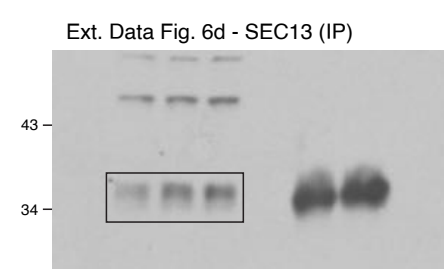
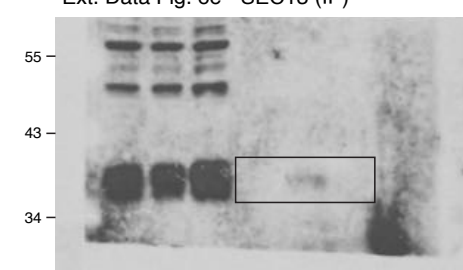
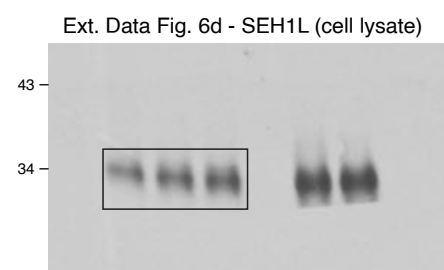
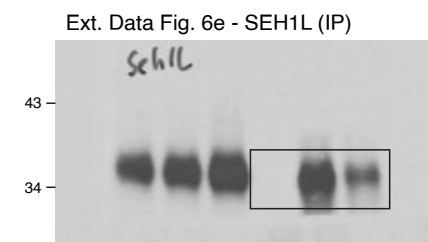
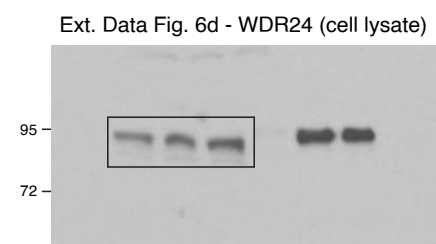
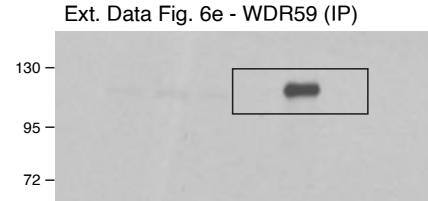
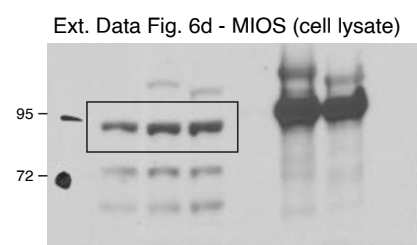
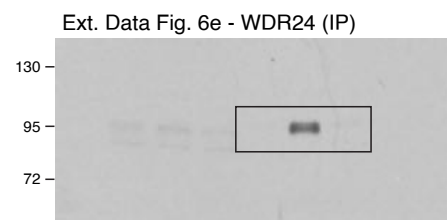
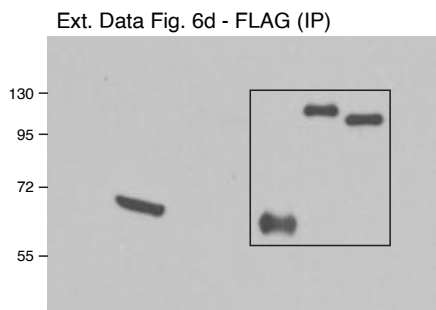
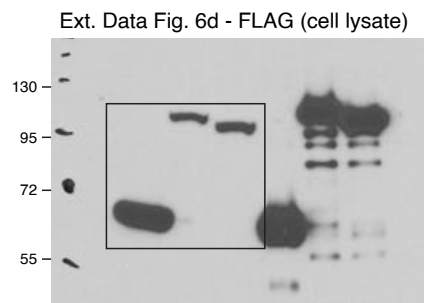
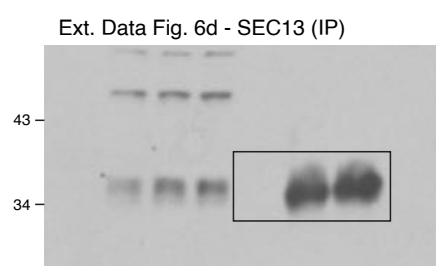
Supplementary Figure 1 | part 7



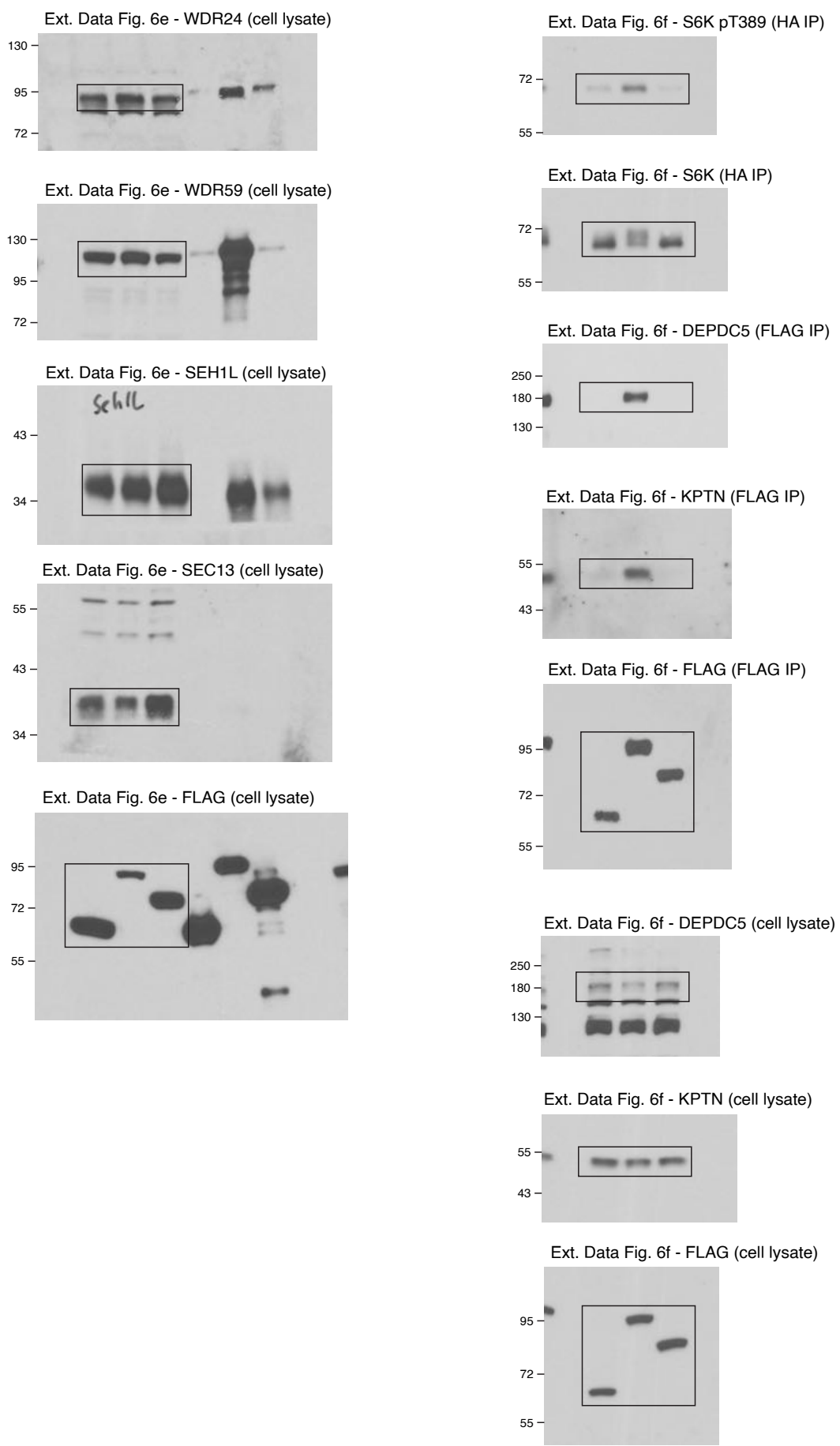
Supplementary Figure 1 | part 8



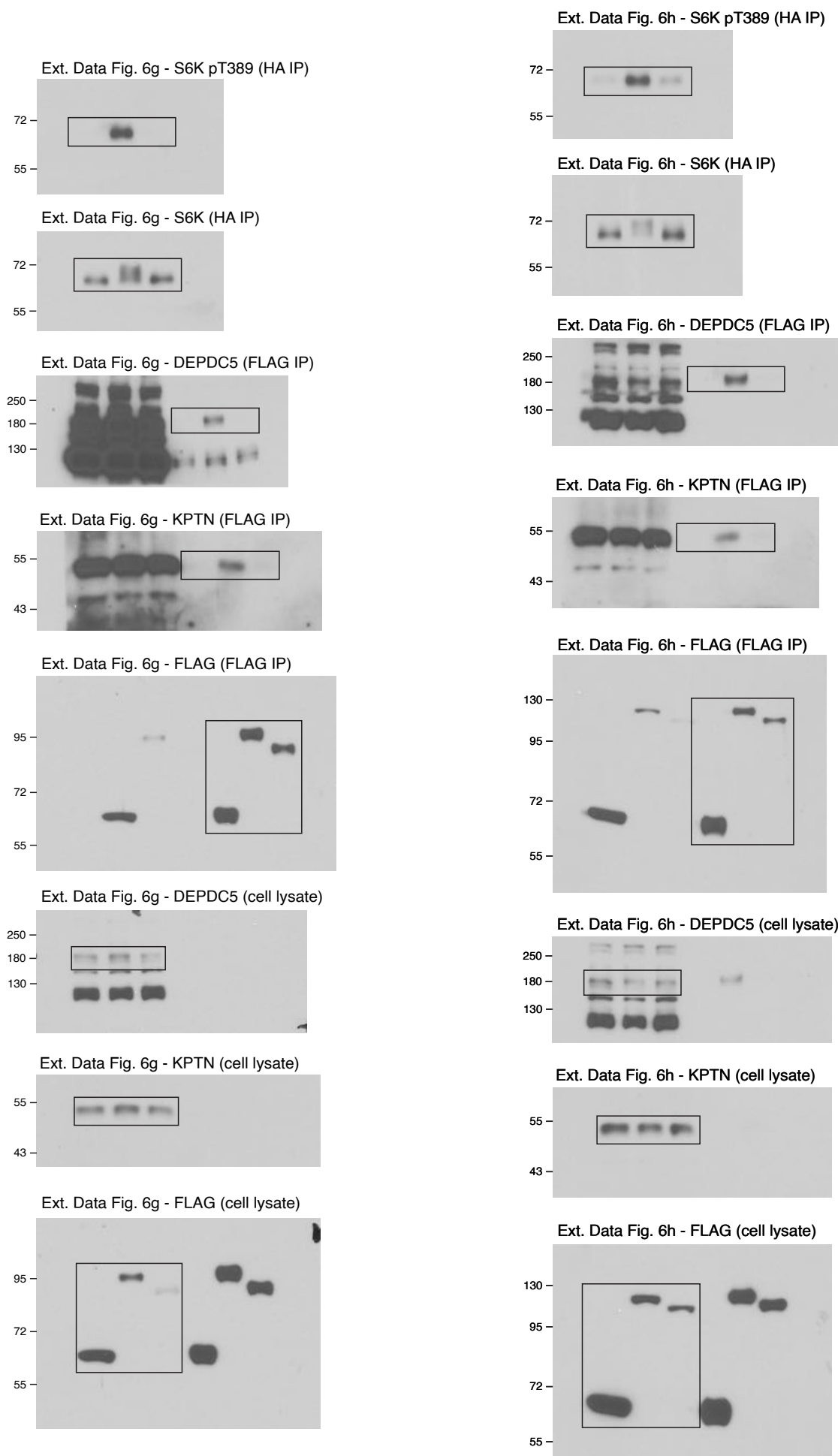
Supplementary Figure 1 | part 9



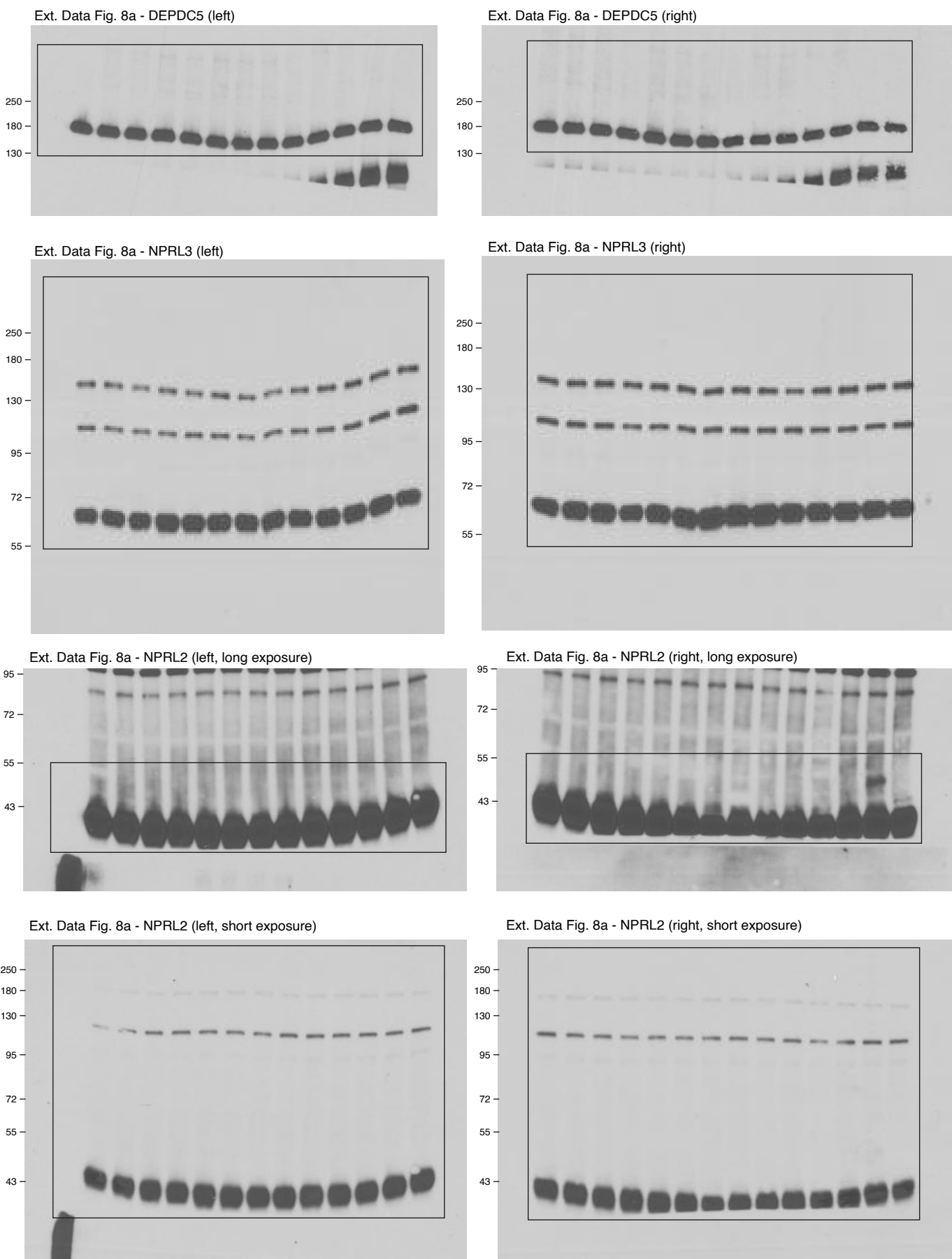
Supplementary Figure 1 | part 10



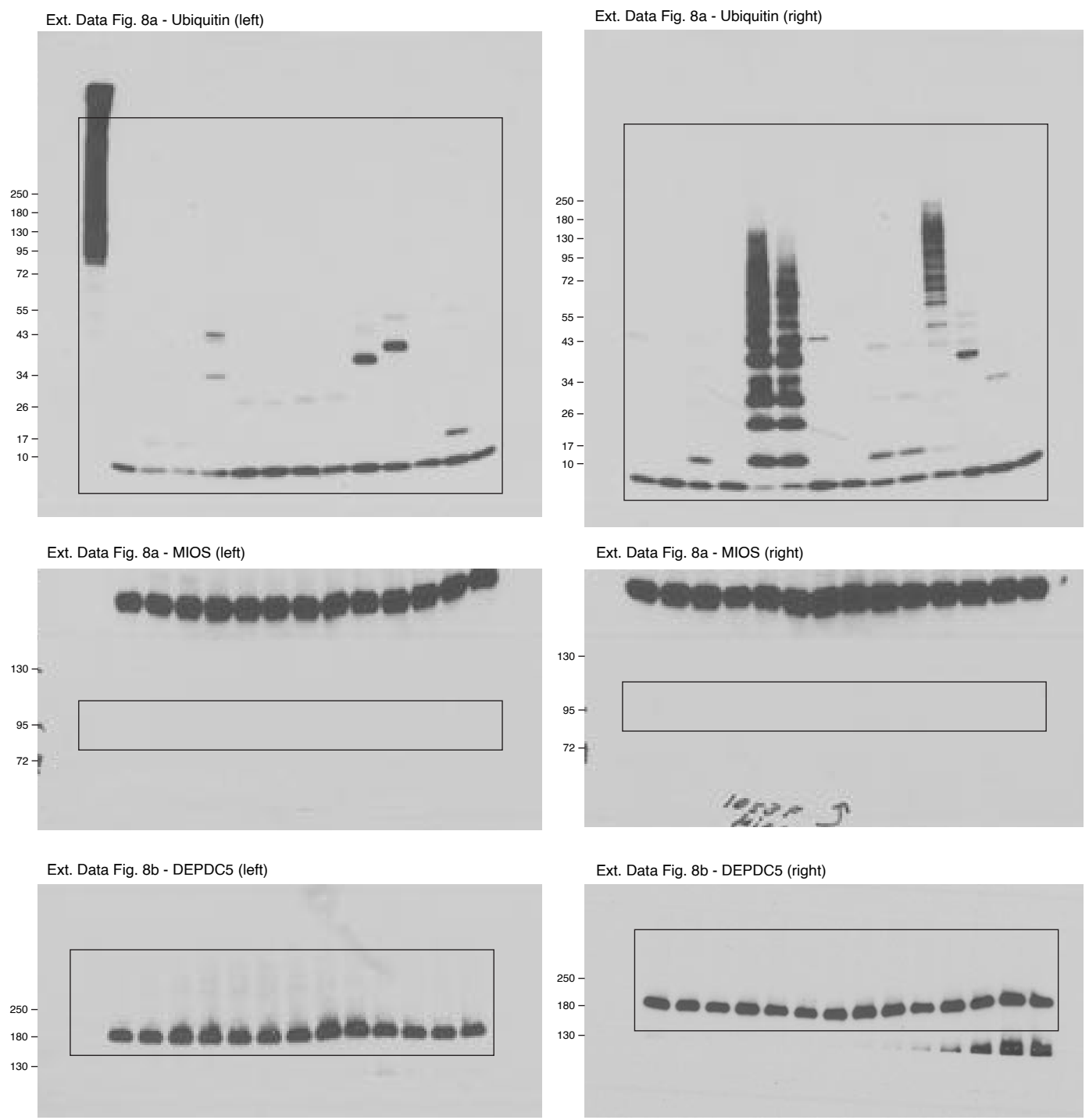
Supplementary Figure 1 | part 11



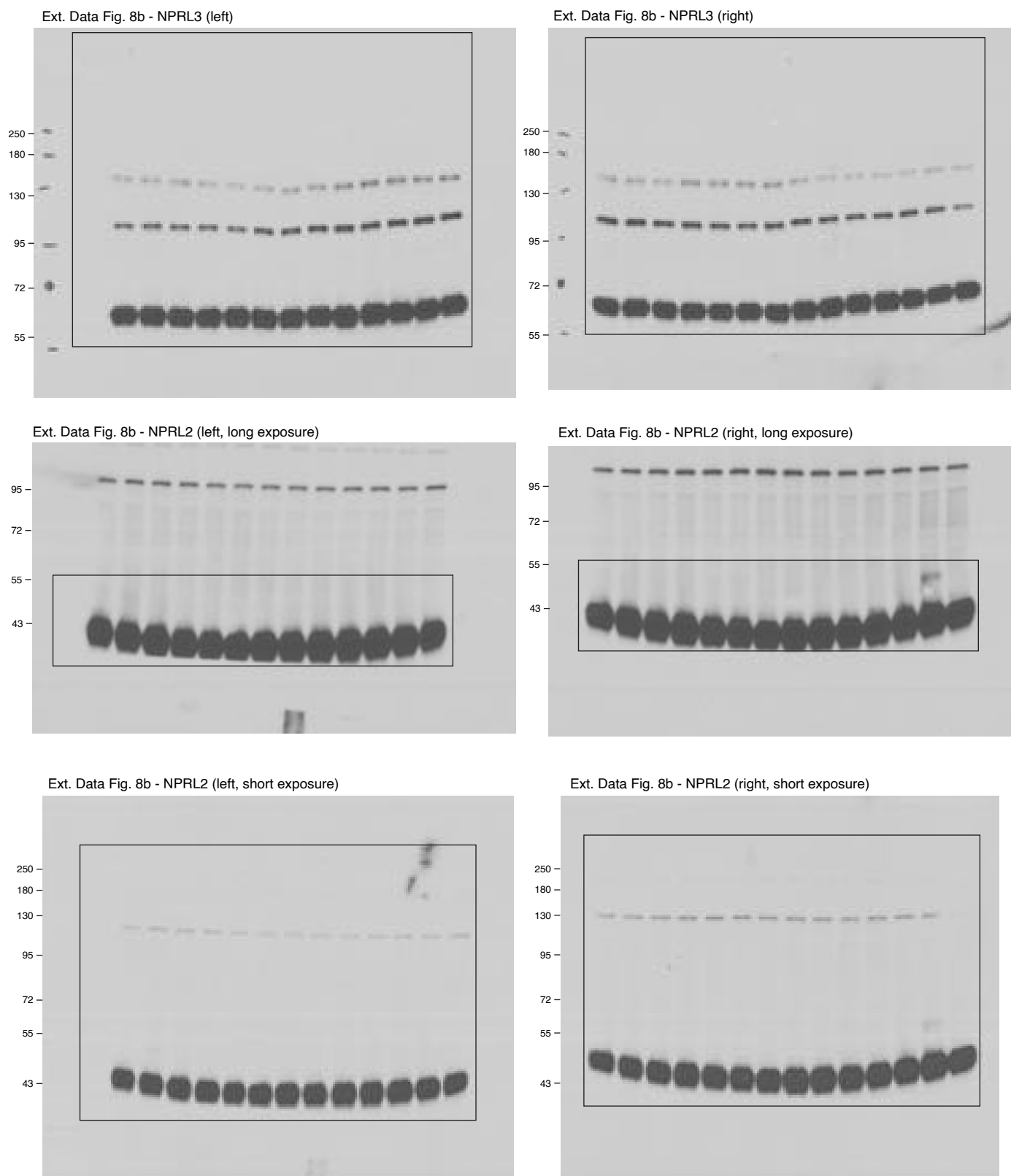
Supplementary Figure 1 | part 12



Supplementary Figure 1 | part 13

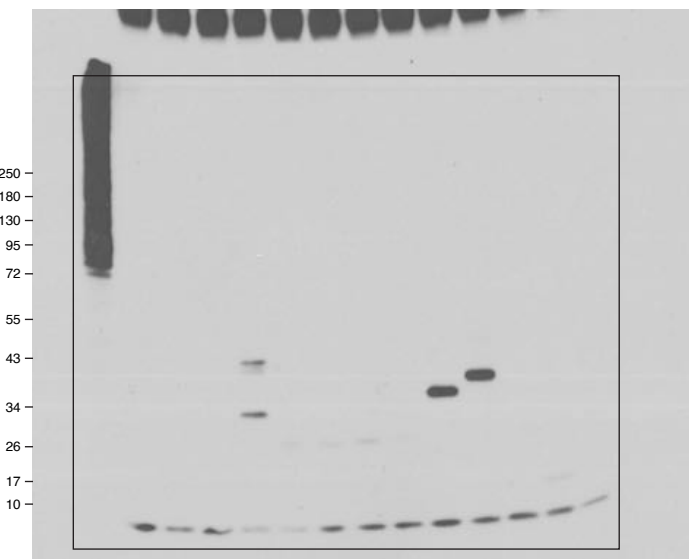


Supplementary Figure 1 | part 14

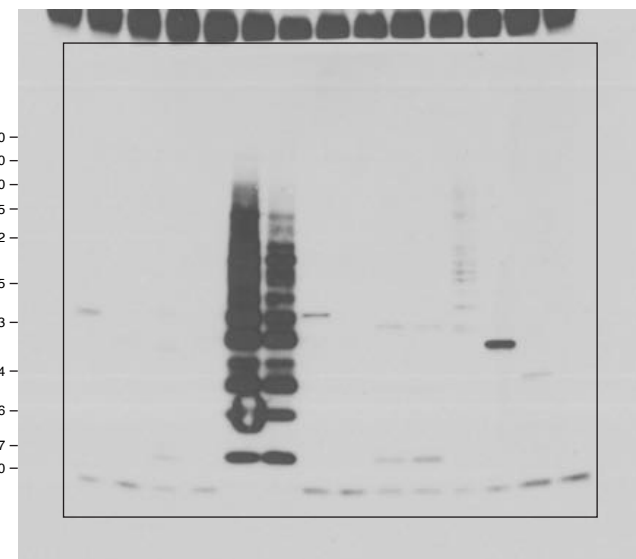


Supplementary Figure 1 | part 15

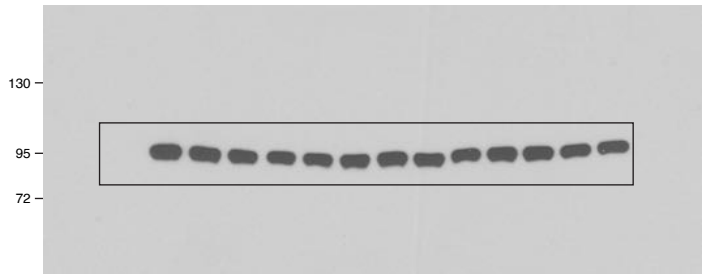
Ext. Data Fig. 8b - Ubiquitin (left)



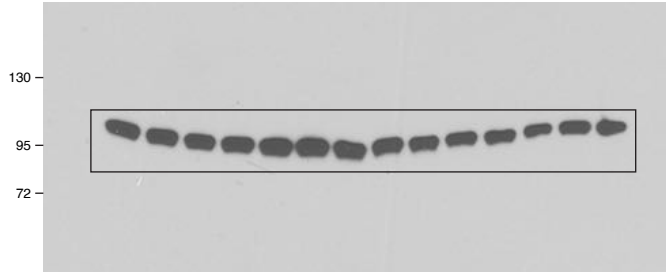
Ext. Data Fig. 8b - Ubiquitin (right)



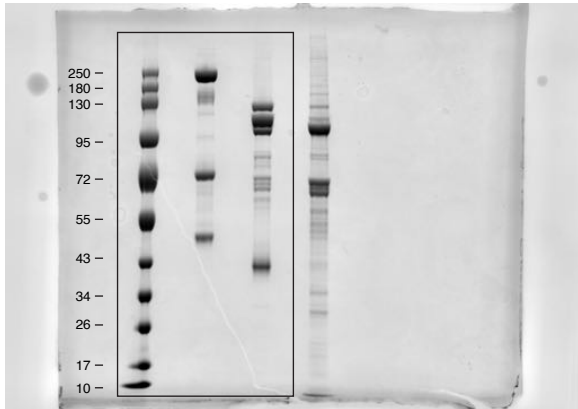
Ext. Data Fig. 8b - MIOS (left)



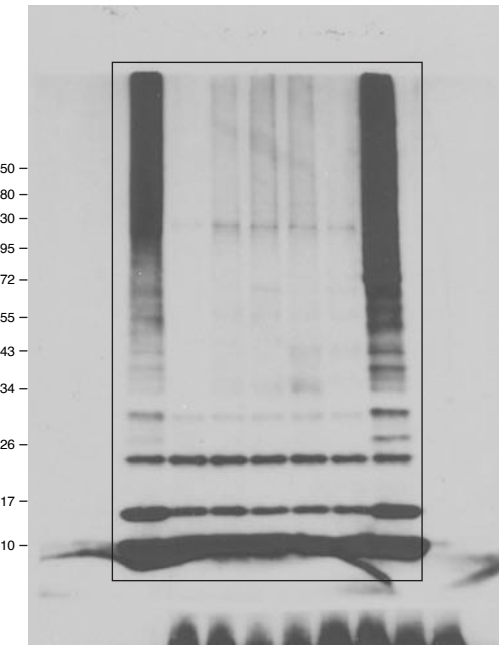
Ext. Data Fig. 8b - MIOS (right)



Ext. Data Fig. 8c - Coomassie

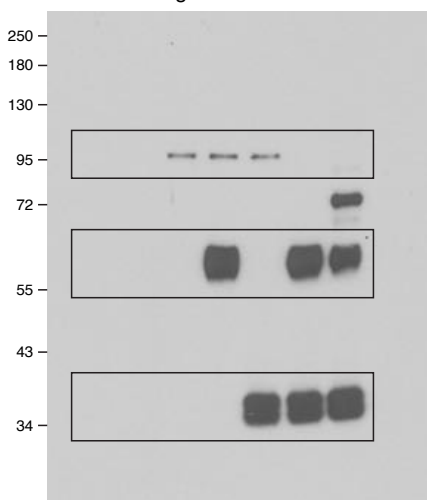


Ext. Data Fig. 8d - Ubiquitin

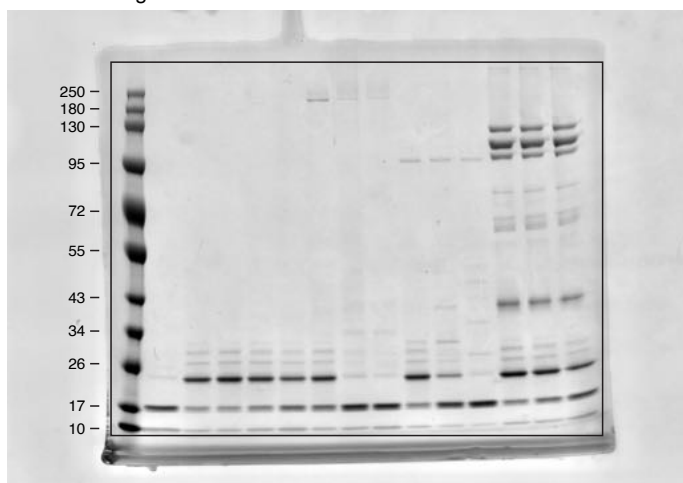


Supplementary Figure 1 | part 16

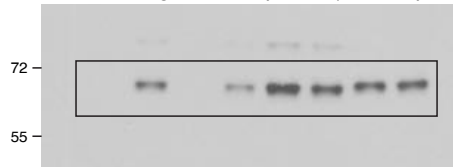
Ext. Data Fig. 8d - FLAG



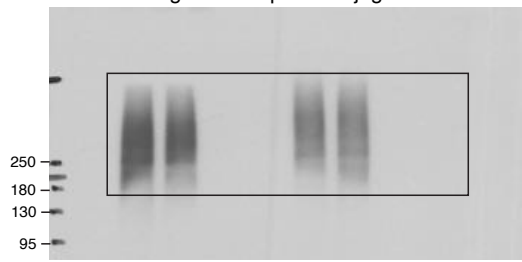
Ext. Data Fig. 8e - Coomassie



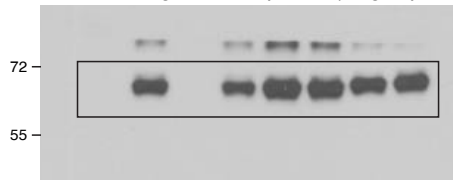
Ext. Data Fig. 8f - S6K pT389 (short exposure)



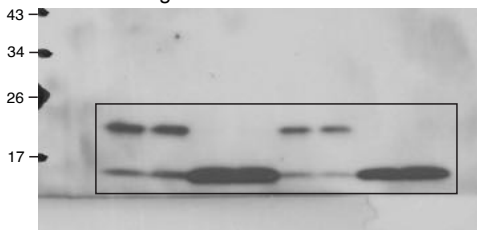
Ext. Data Fig. 8f - Ubiquitin conjugates



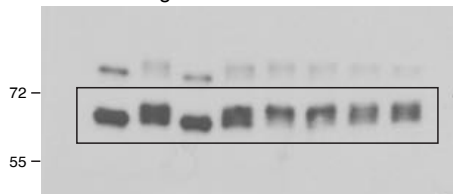
Ext. Data Fig. 8f - S6K pT389 (long exposure)



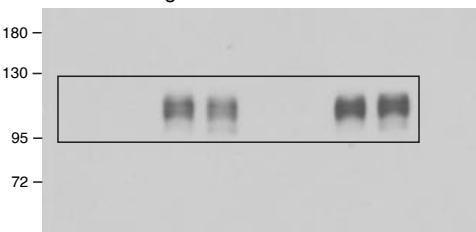
Ext. Data Fig. 8f - UBE2D



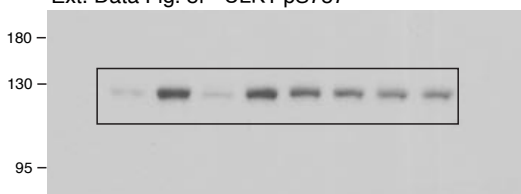
Ext. Data Fig. 8f - S6K



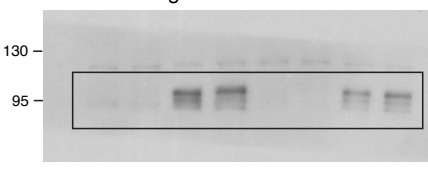
Ext. Data Fig. 8f - HIF1α



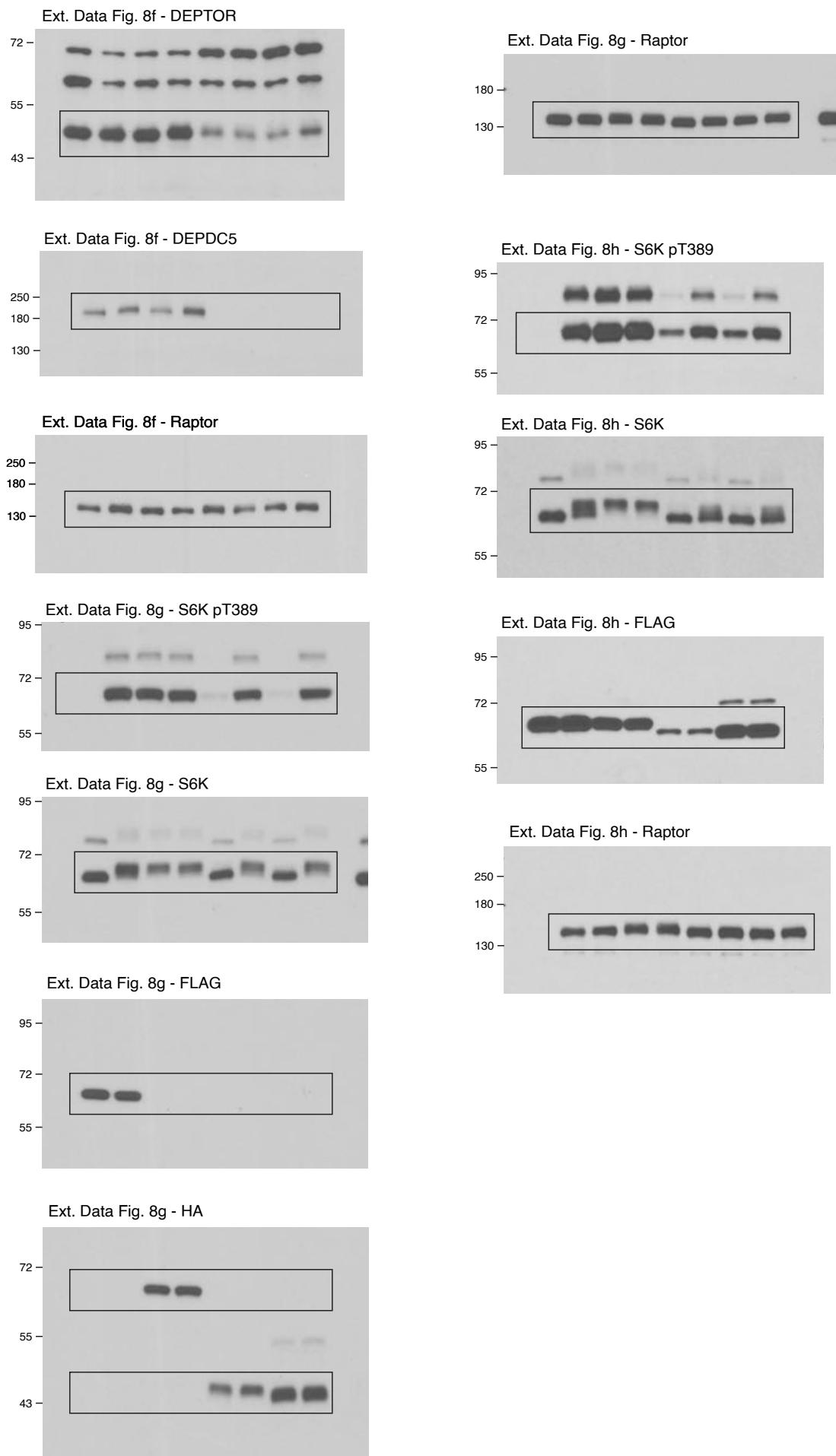
Ext. Data Fig. 8f - ULK1 pS757



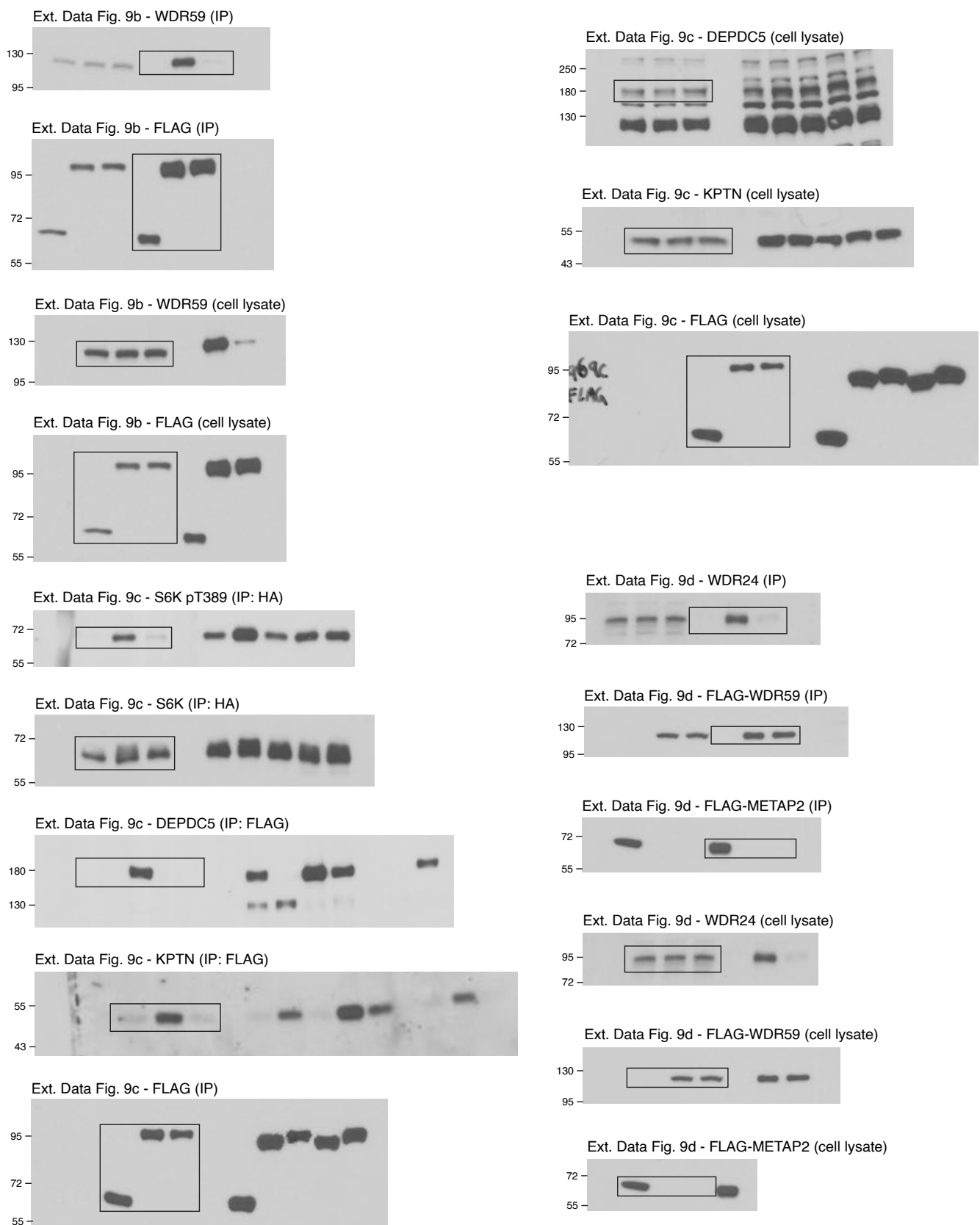
Ext. Data Fig. 8f - NRF2



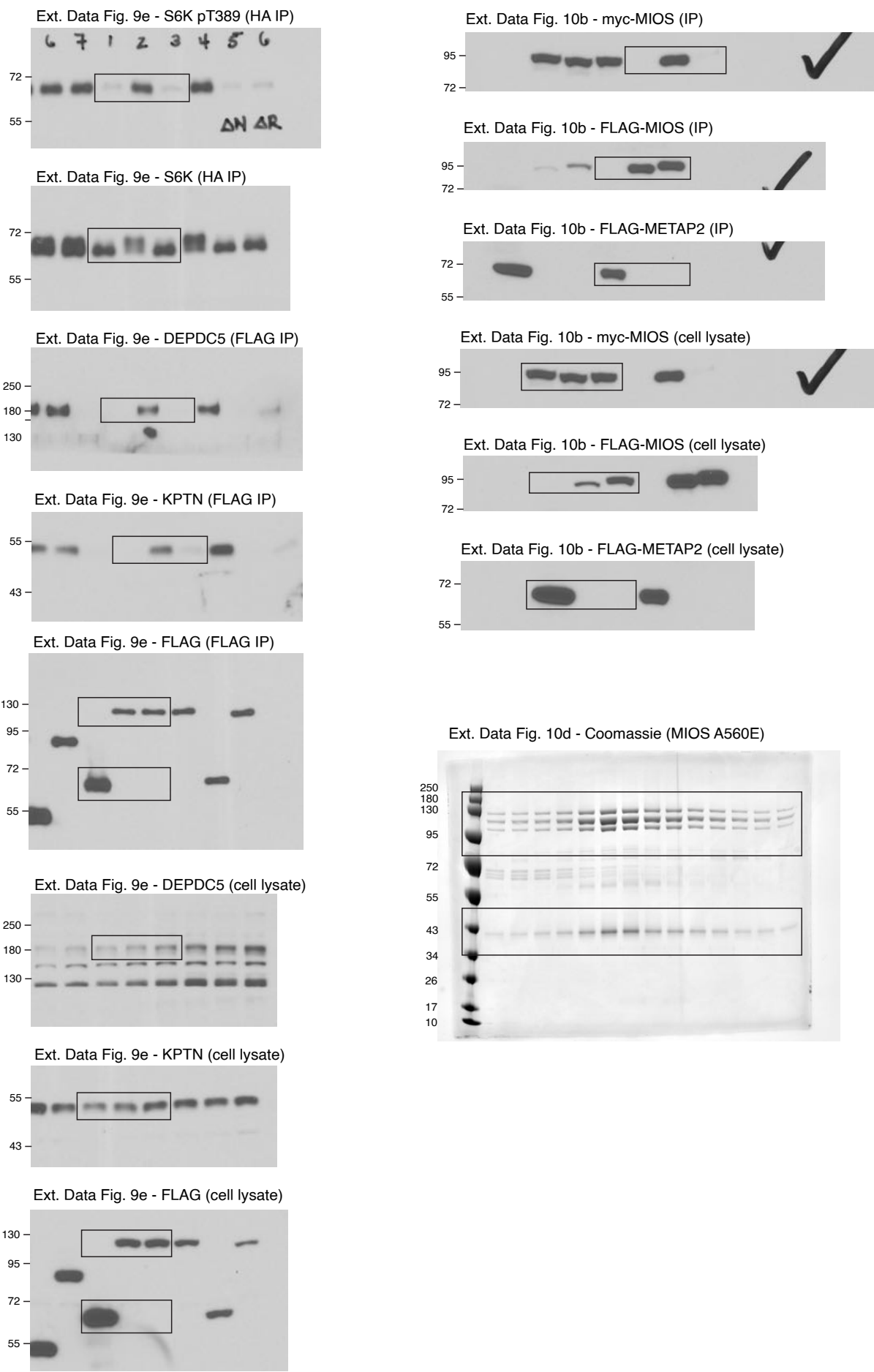
Supplementary Figure 1 | part 17



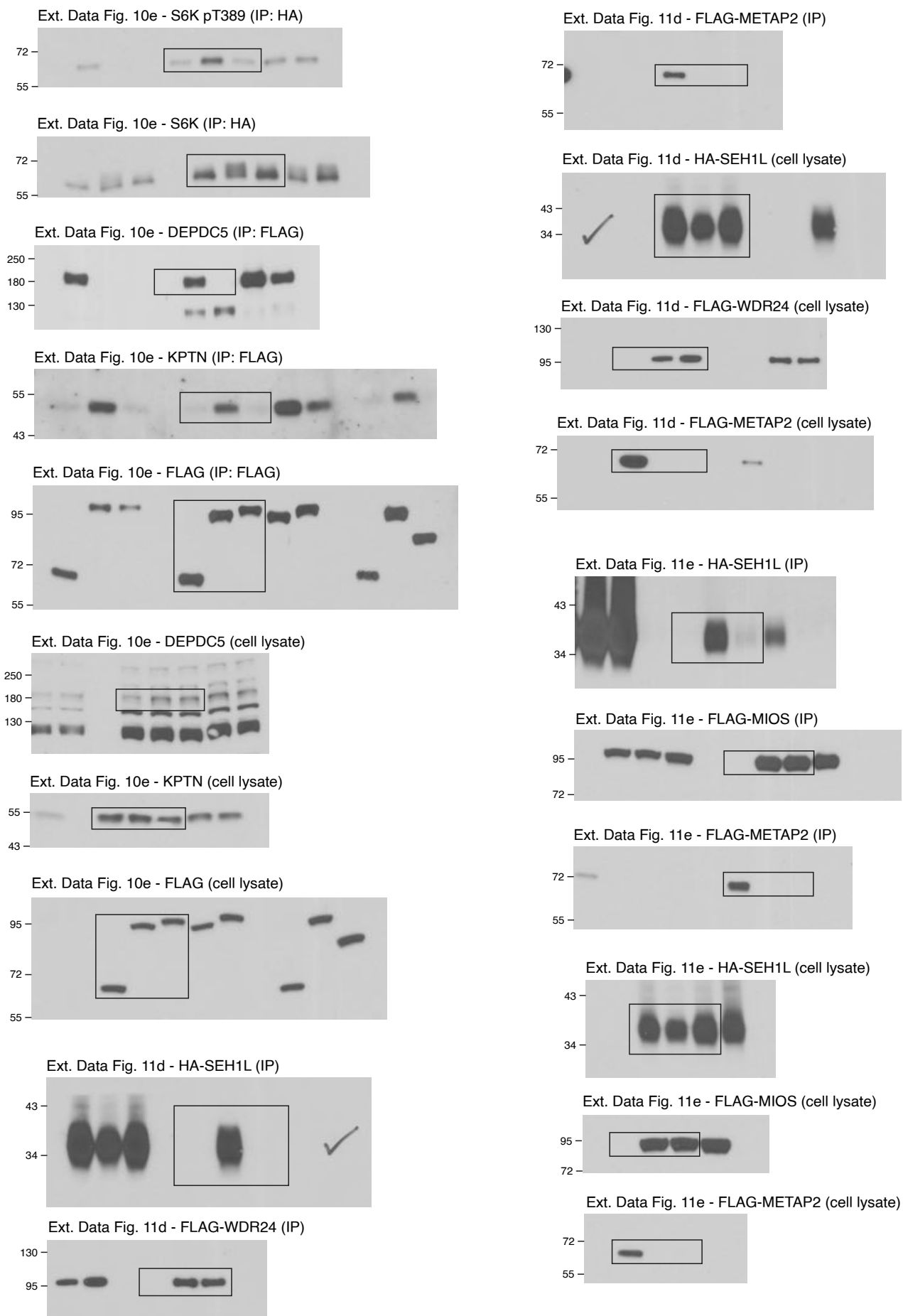
Supplementary Figure 1 | part 18



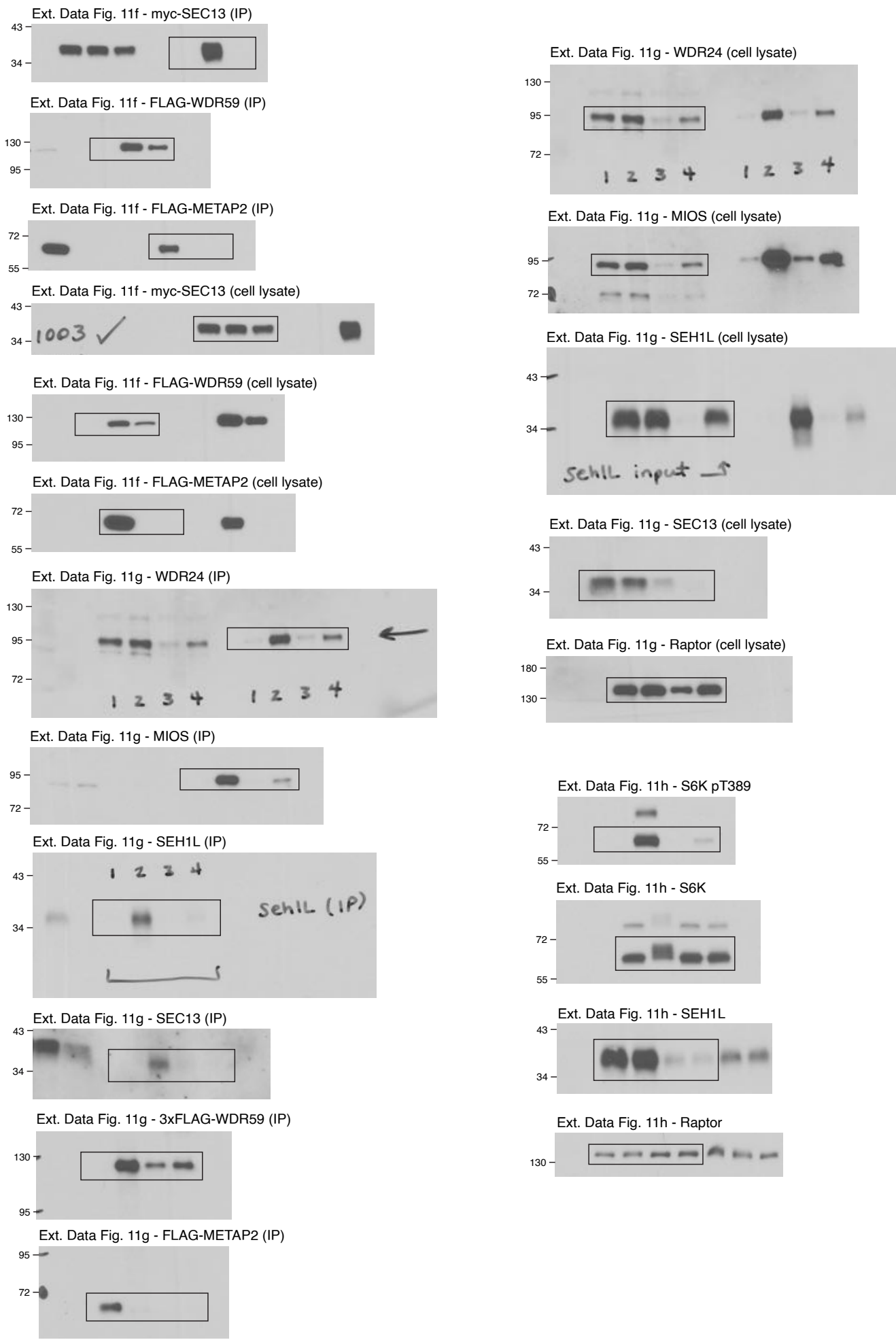
Supplementary Figure 1 | part 19



Supplementary Figure 1 | part 20

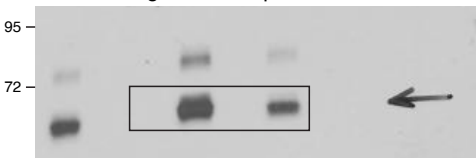


Supplementary Figure 1 | part 21



Supplementary Figure 1 | part 22

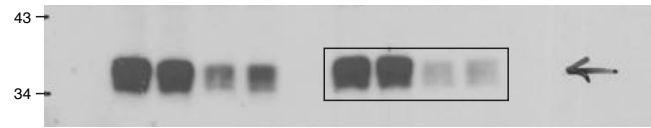
Ext. Data Fig. 11i - S6K pT389



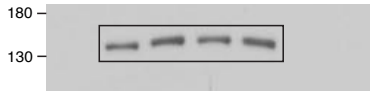
Ext. Data Fig. 11i - S6K



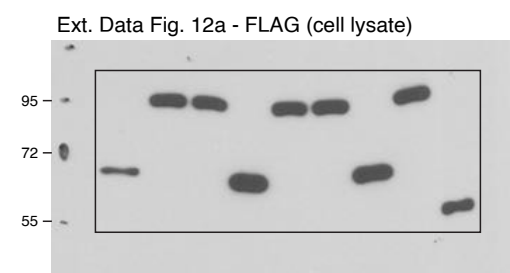
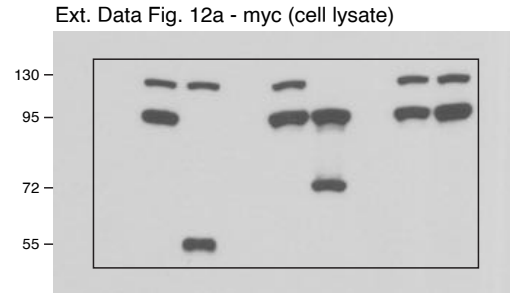
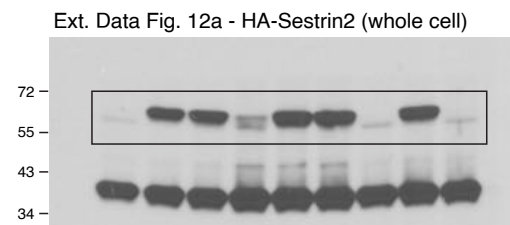
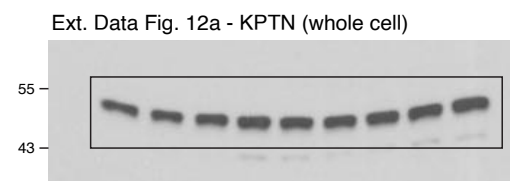
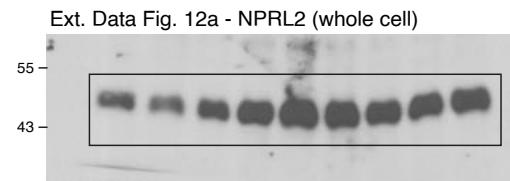
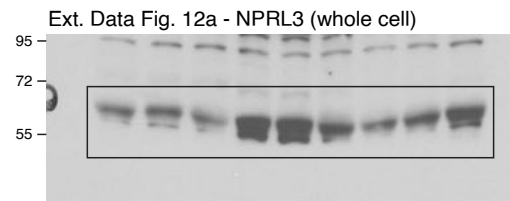
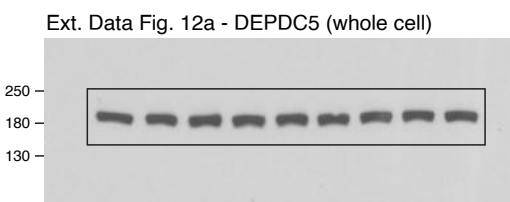
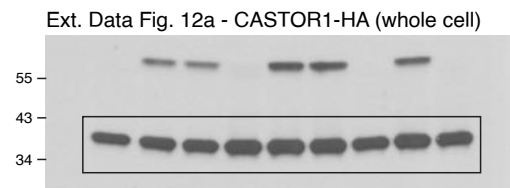
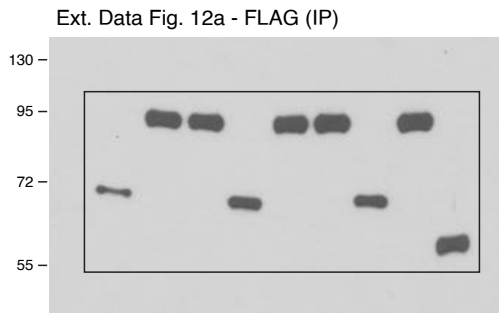
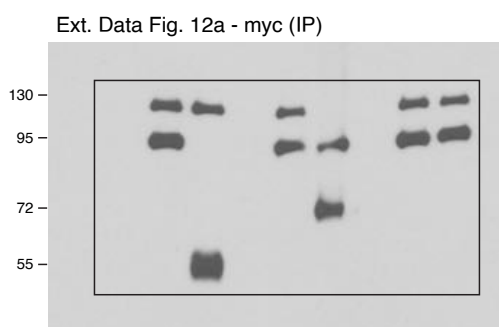
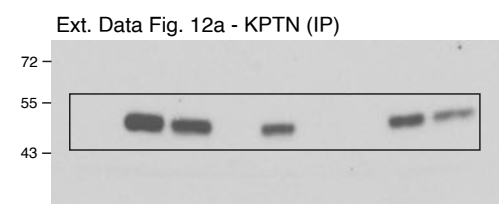
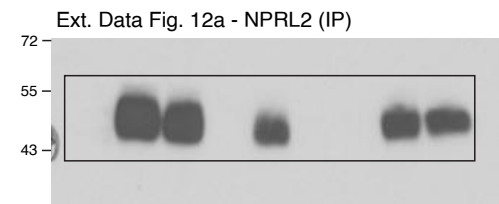
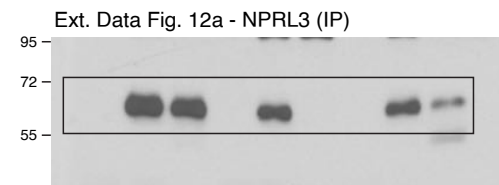
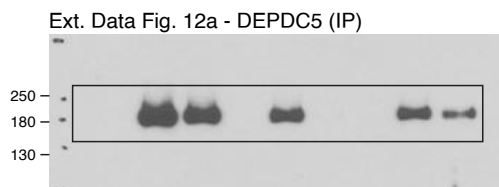
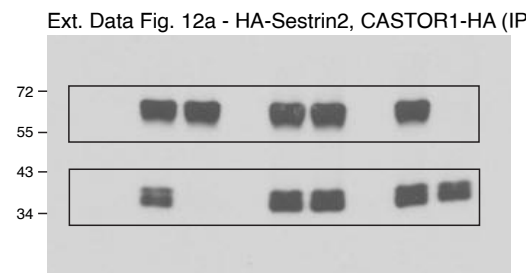
Ext. Data Fig. 11i - SEC13



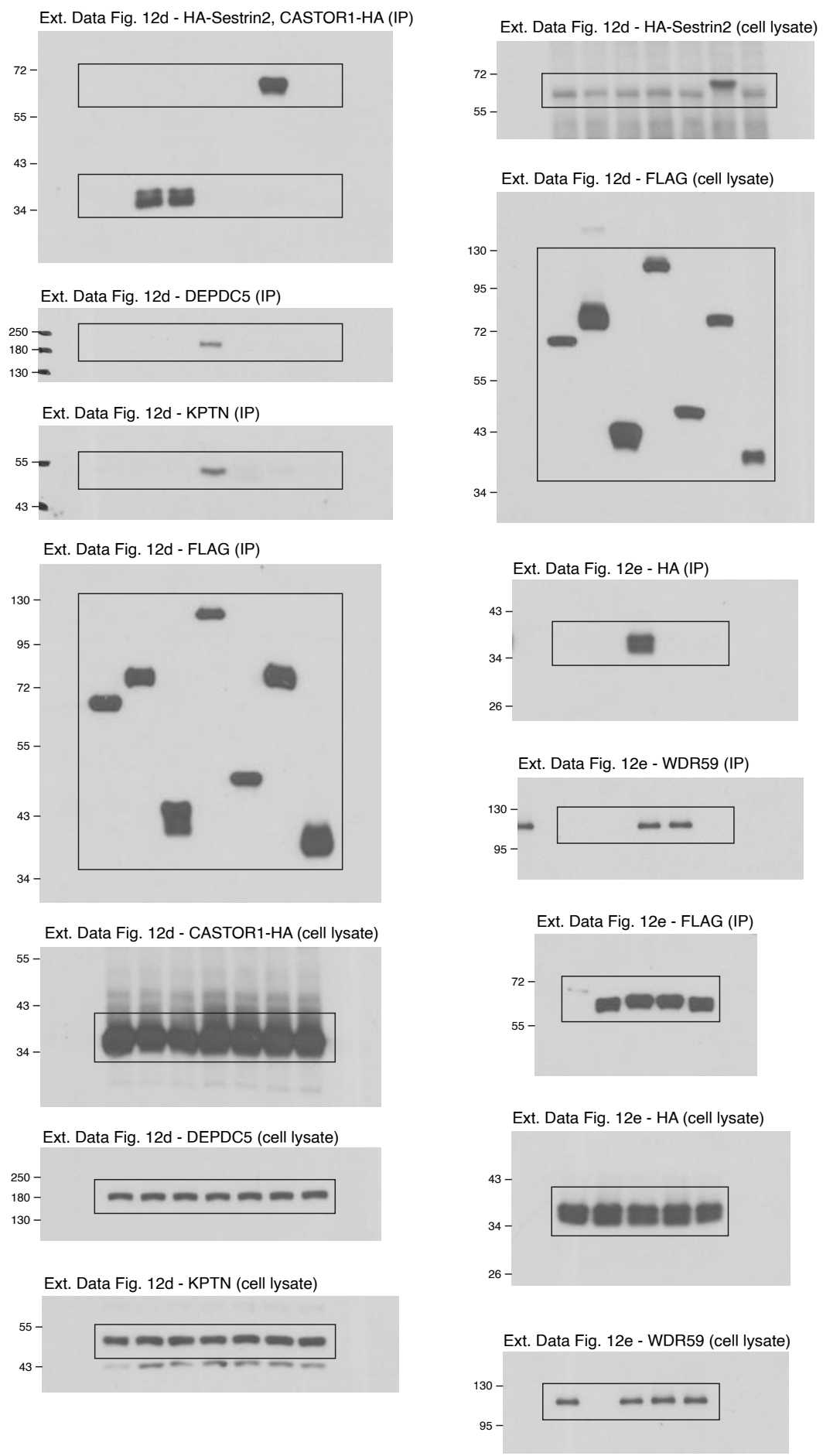
Ext. Data Fig. 11i - Raptor



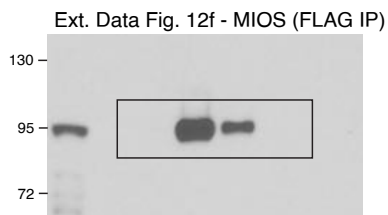
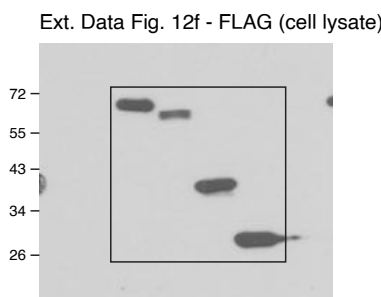
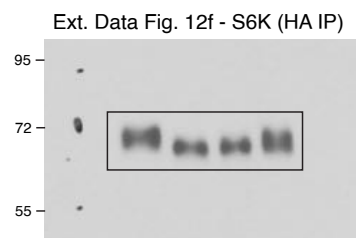
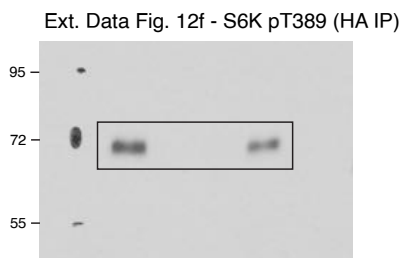
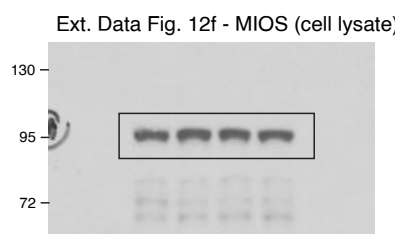
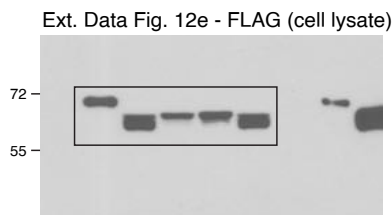
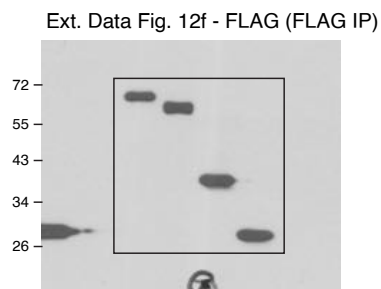
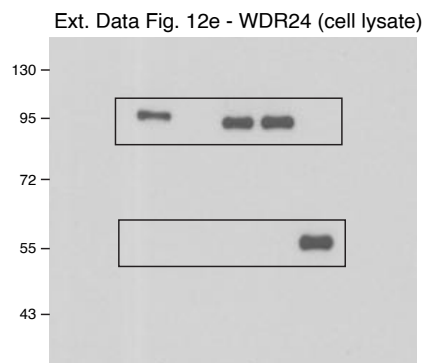
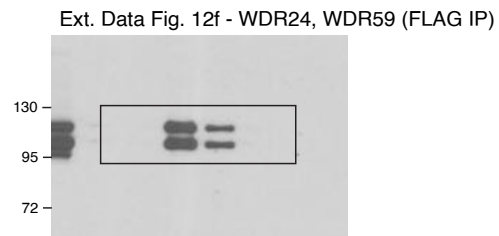
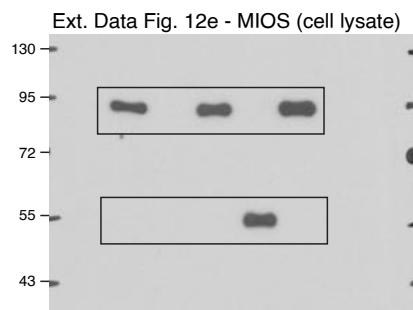
Supplementary Figure 1 | part 23



Supplementary Figure 1 | part 24

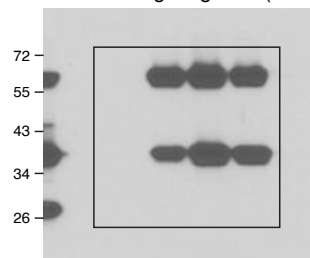


Supplementary Figure 1 | part 25

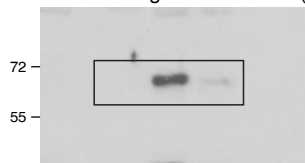


Supplementary Figure 1 | part 26

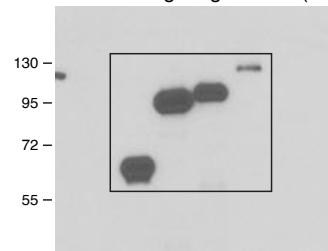
Ext. Data Fig. 12g - HA (FLAG IP)



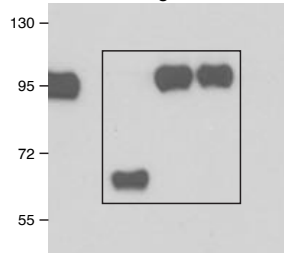
Ext. Data Fig. 12h - NPRL3 (FLAG IP)



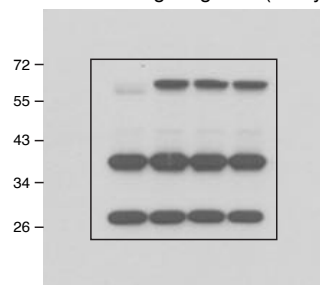
Ext. Data Fig. 12g - FLAG (IP)



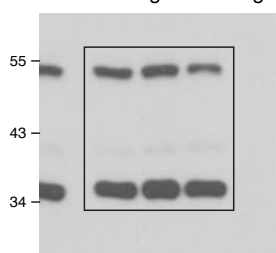
Ext. Data Fig. 12h - FLAG (FLAG IP)



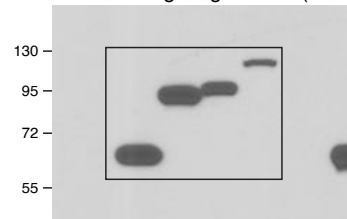
Ext. Data Fig. 12g - HA (cell lysate)



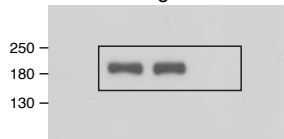
Ext. Data Fig. 12h - RagA, RagC (cell lysate)



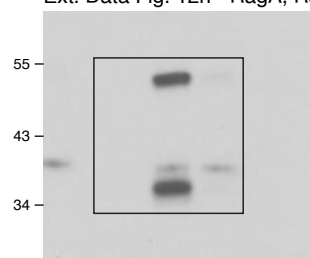
Ext. Data Fig. 12g - FLAG (cell lysate)



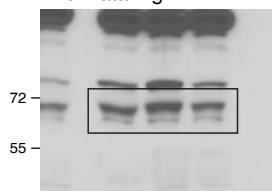
Ext. Data Fig. 12h - DEPDC5 (cell lysate)



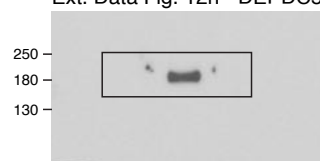
Ext. Data Fig. 12h - RagA, RagC (FLAG IP)



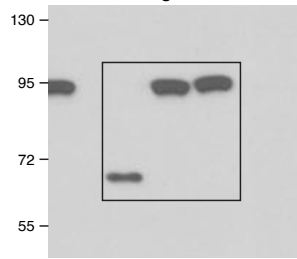
Ext. Data Fig. 12h - NPRL3 (cell lysate)



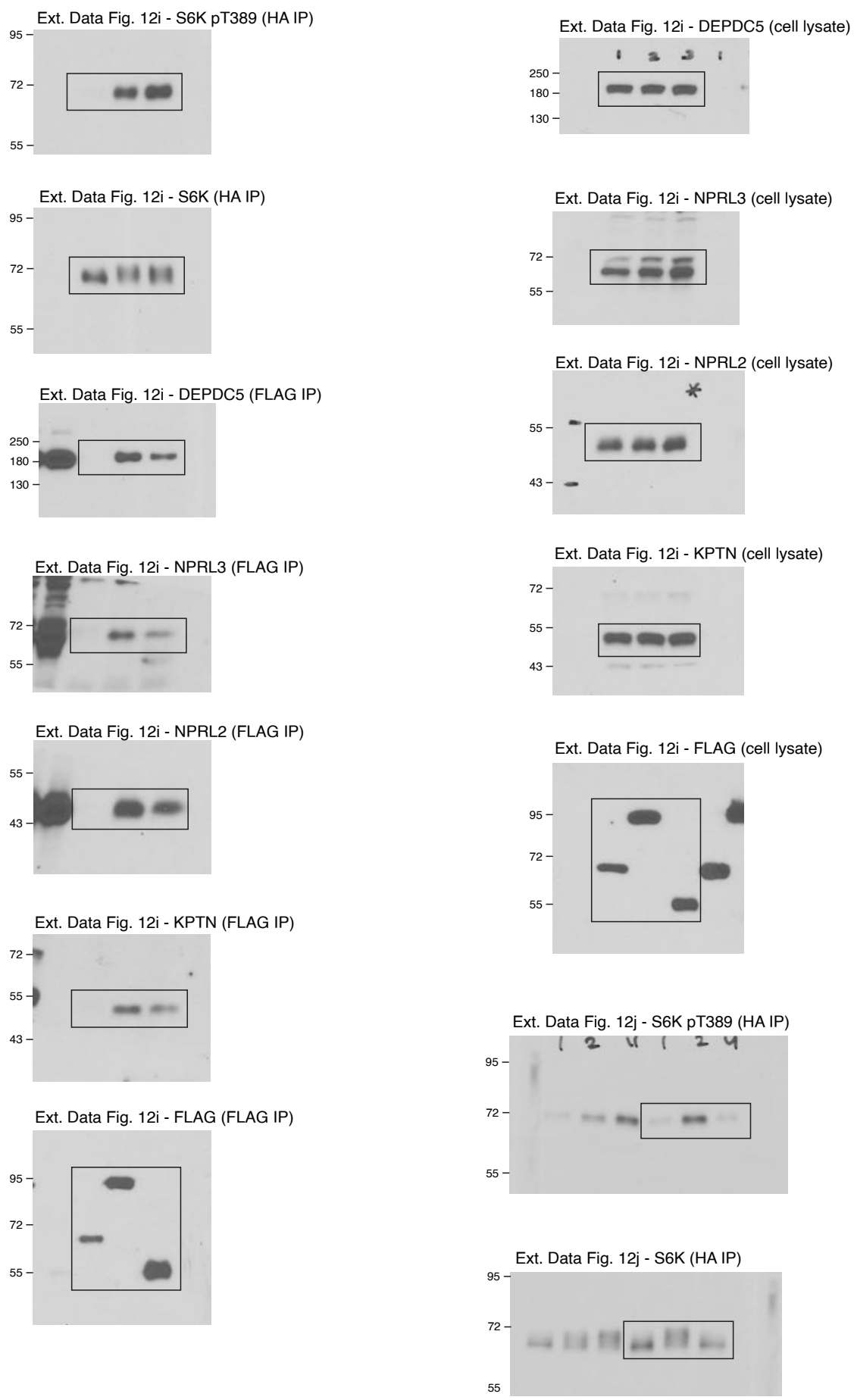
Ext. Data Fig. 12h - DEPDC5 (FLAG IP)



Ext. Data Fig. 12h - FLAG (cell lysate)



Supplementary Figure 1 | part 27

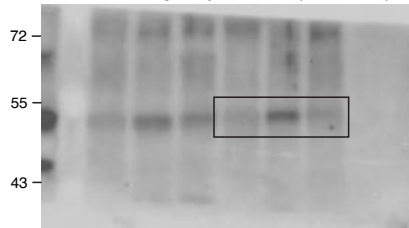


Supplementary Figure 1 | part 28

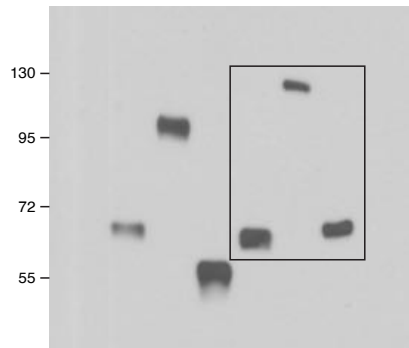
Ext. Data Fig. 12j - DEPDC5 (FLAG IP)



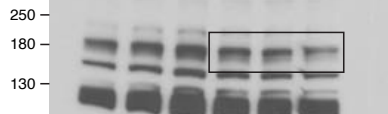
Ext. Data Fig. 12j - KPTN (FLAG IP)



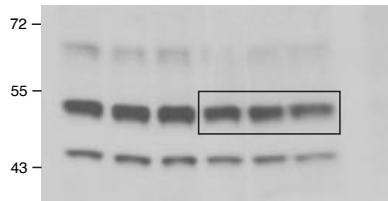
Ext. Data Fig. 12j - FLAG (FLAG IP)



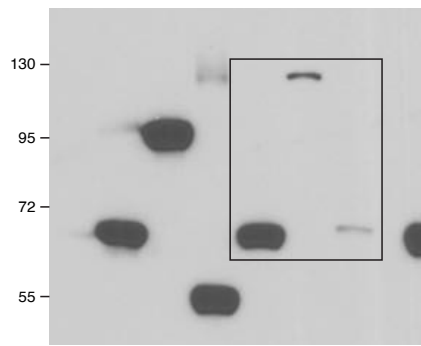
Ext. Data Fig. 12j - DEPDC5 (cell lysate)



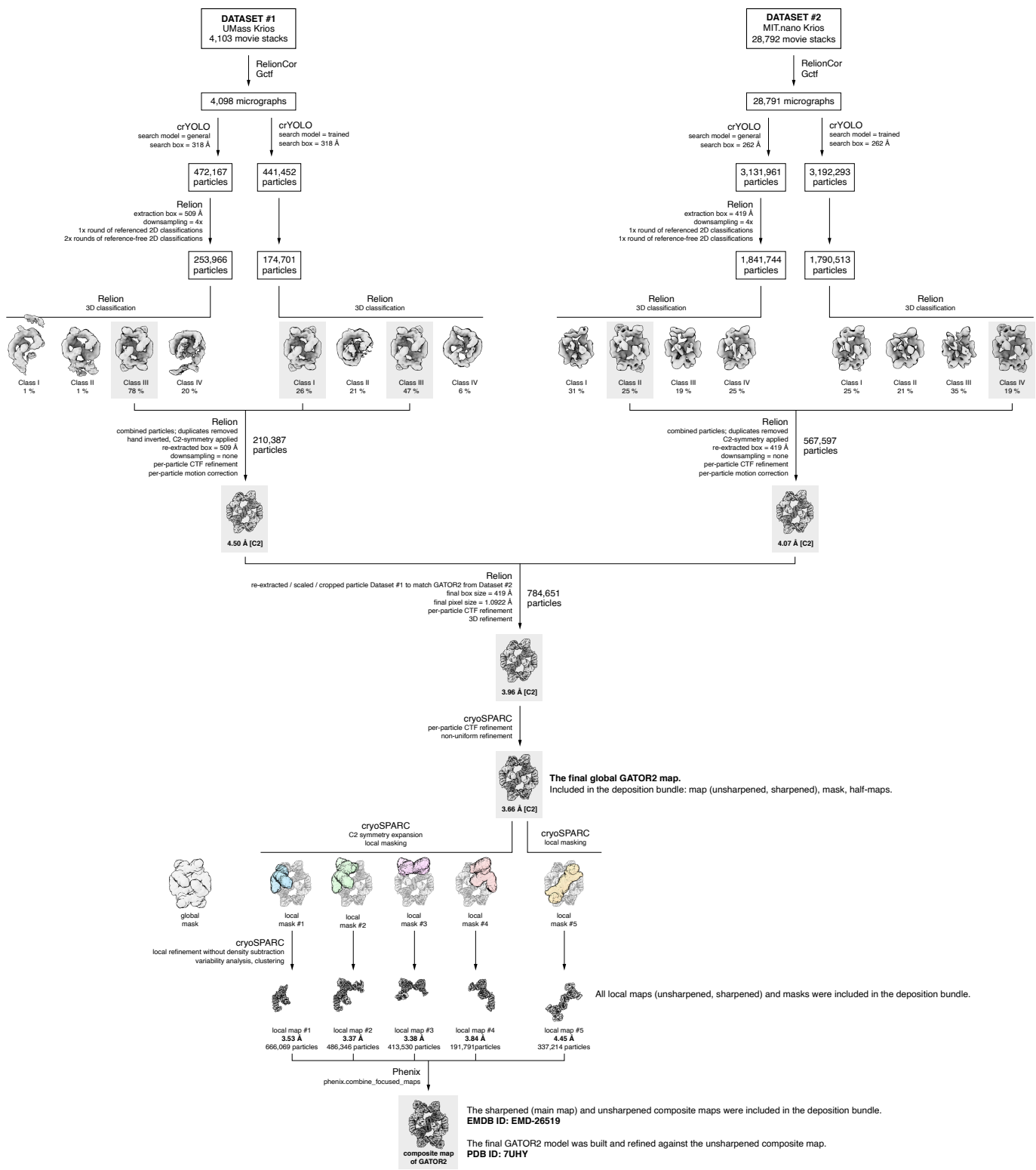
Ext. Data Fig. 12j - KPTN (cell lysate)



Ext. Data Fig. 12j - FLAG (cell lysate)

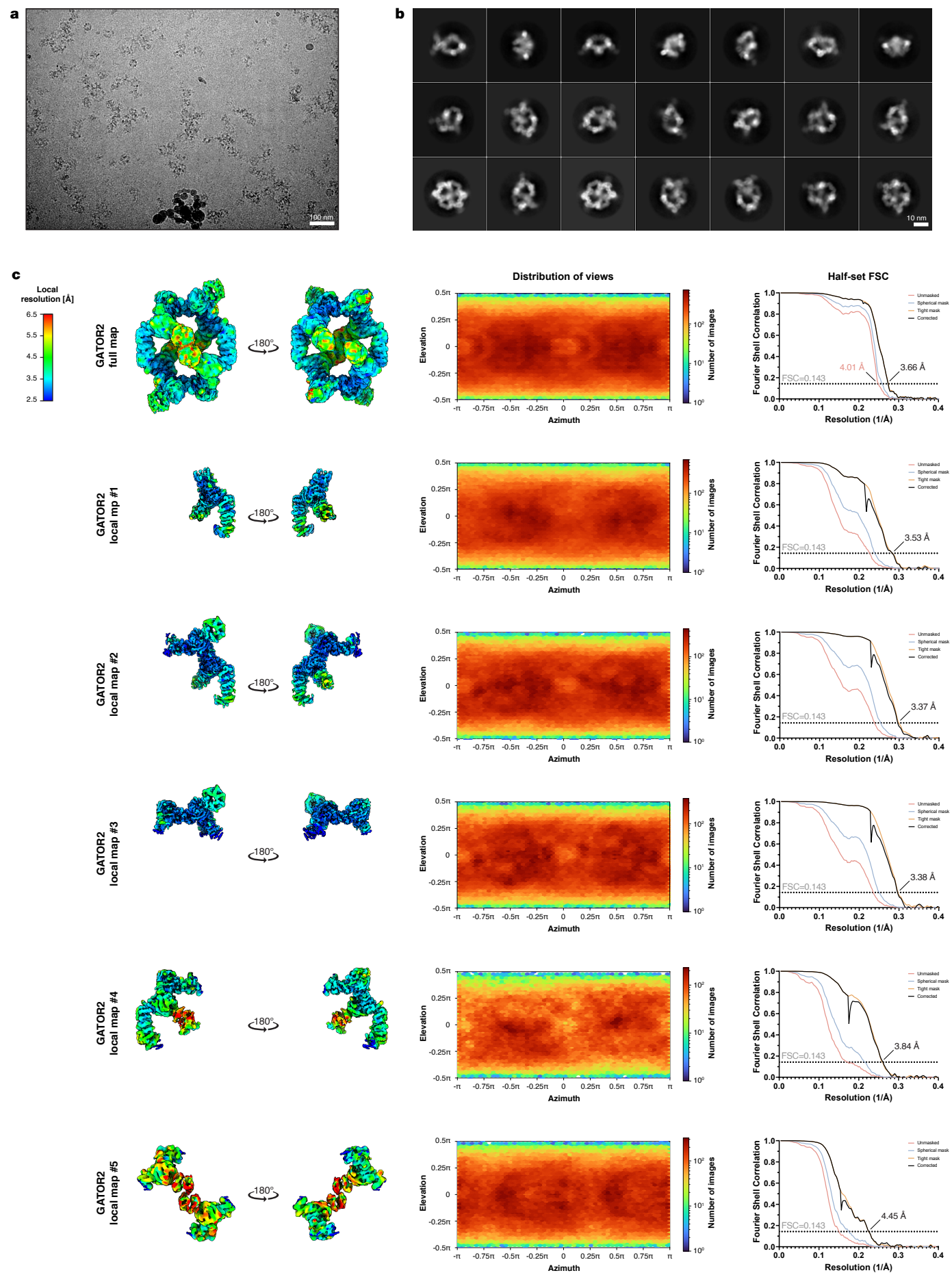


Supplementary Figure 2



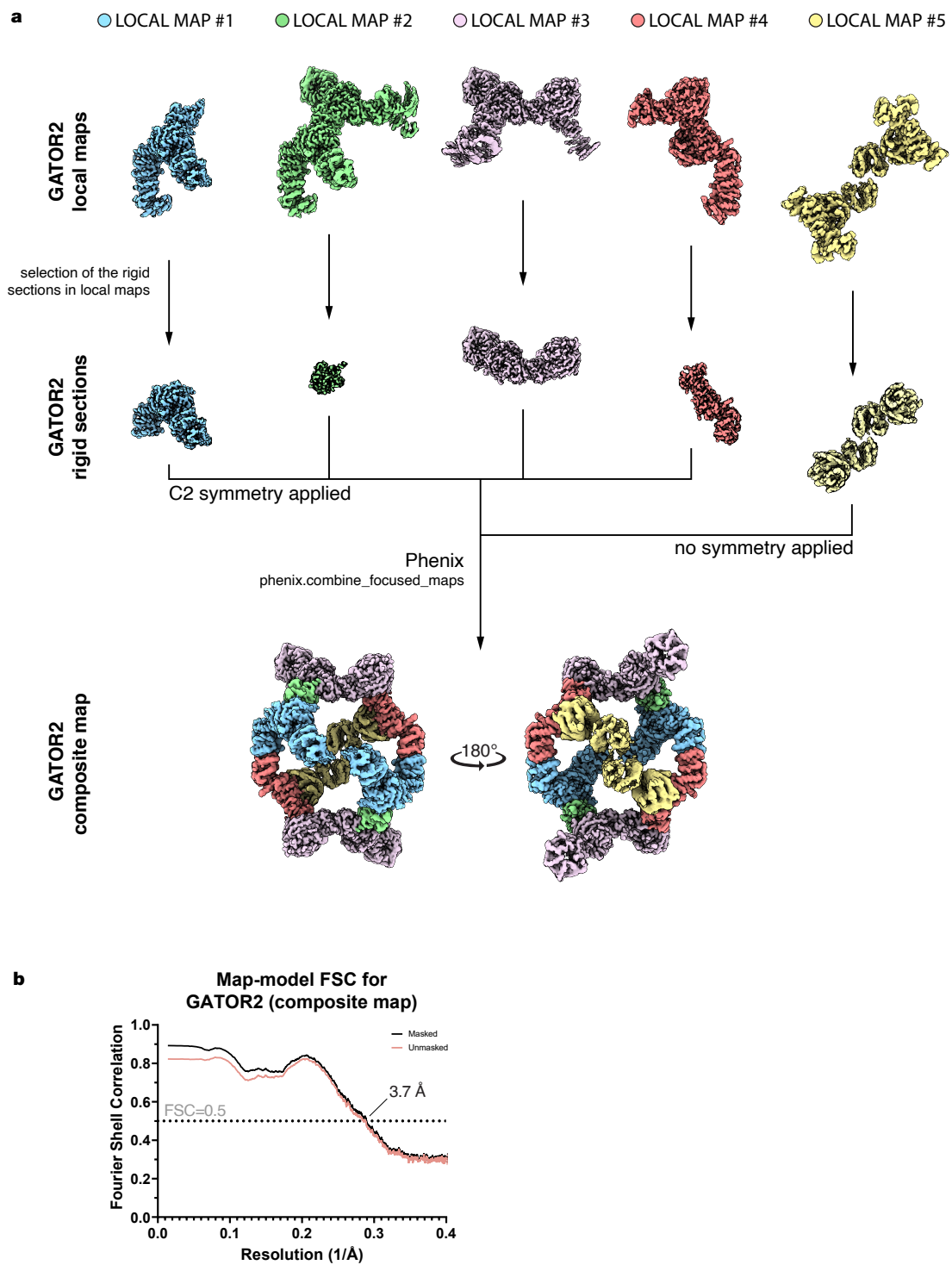
Supplementary Fig. 2 | Cryo-EM data collection and processing. Workflow for data collection and processing of the GATOR2 datasets.

Supplementary Figure 3



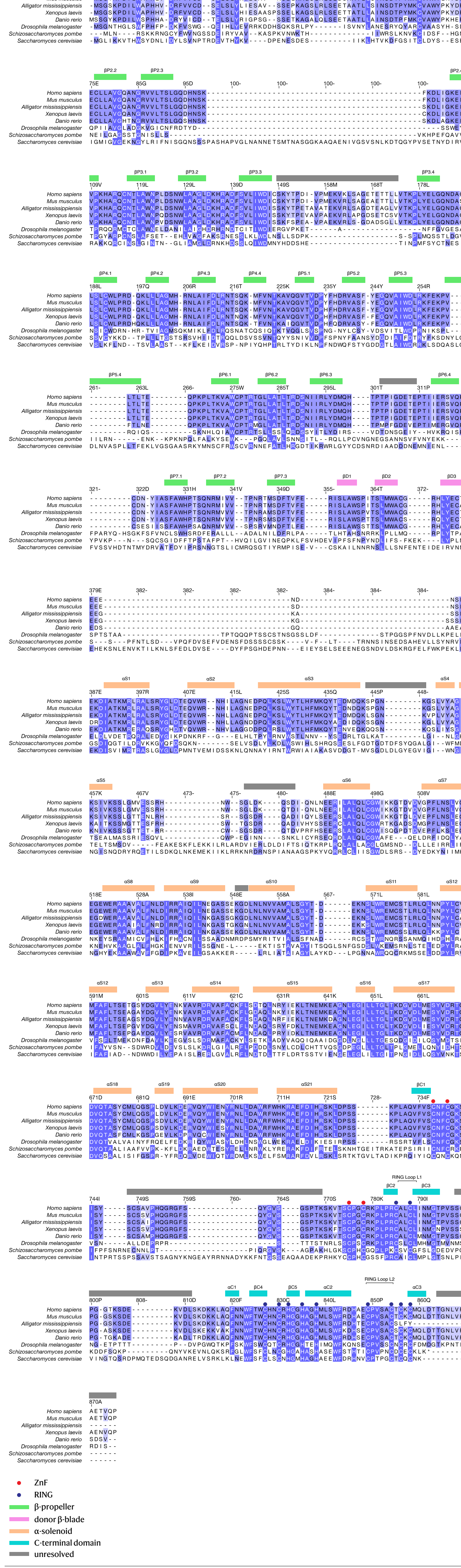
Supplementary Fig. 3 | Structural determination of GATOR2. **a**, Representative micrograph of grids spotted with GATOR2. **b**, Representative two-dimensional class averages of the GATOR2 complex. **c**, Local resolution, view angle distribution, and half-set gold-standard Fourier shell correlation (FCS) for the full GATOR2 map (top) and local maps used for generation of a composite map.

Supplementary Figure 4



Supplementary Fig. 4 | Generation of a composite GATOR2 map. **a**, Flowchart depicting the assembly of a composite, high occupancy, GATOR2 map from rigid sections of local maps. **b**, Map-model FSC for the GATOR2 composite map.

Supplementary Figure S

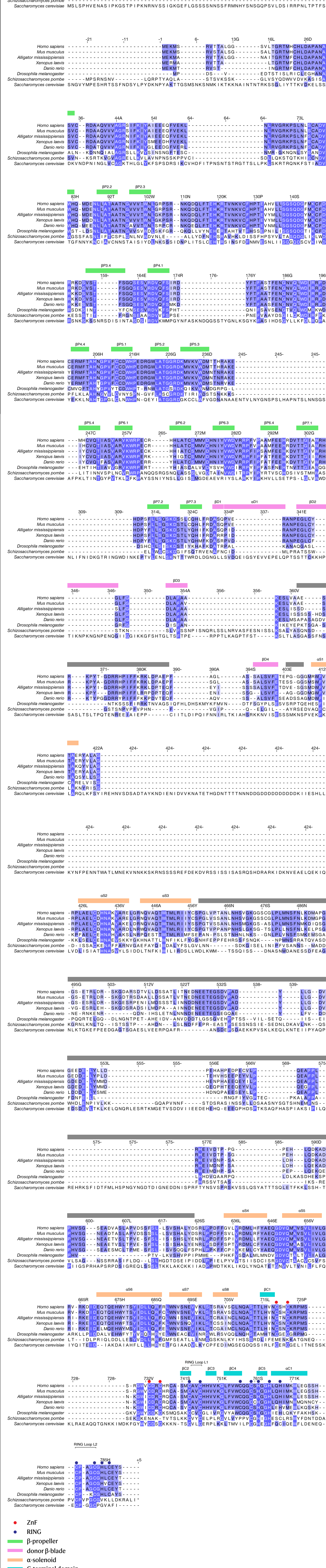


- Supplementary Fig. 3 | Sequence**
Numbering refers to the human residues that participate in the o-EM structure.

33 | Nature | **Vaishnava and Rogala et al. (2022)** | <https://doi.org/10.1038/s41586-022-04559-2>

WDR24

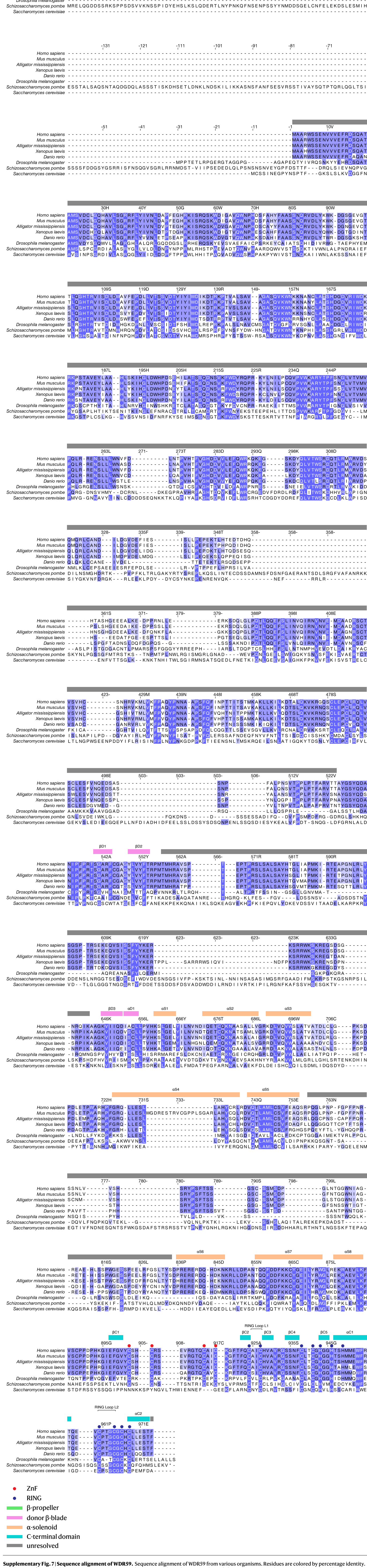
Alligator m.



Supplementary Fig. 6 | Sequence alignment of WDR24. Sequence alignment of WDR24 from various organisms. Residues are colored by percentage identity. Numbering refers to the human protein sequence. Secondary structure boundaries are indicated above the sequence alignment and are colored by domain.

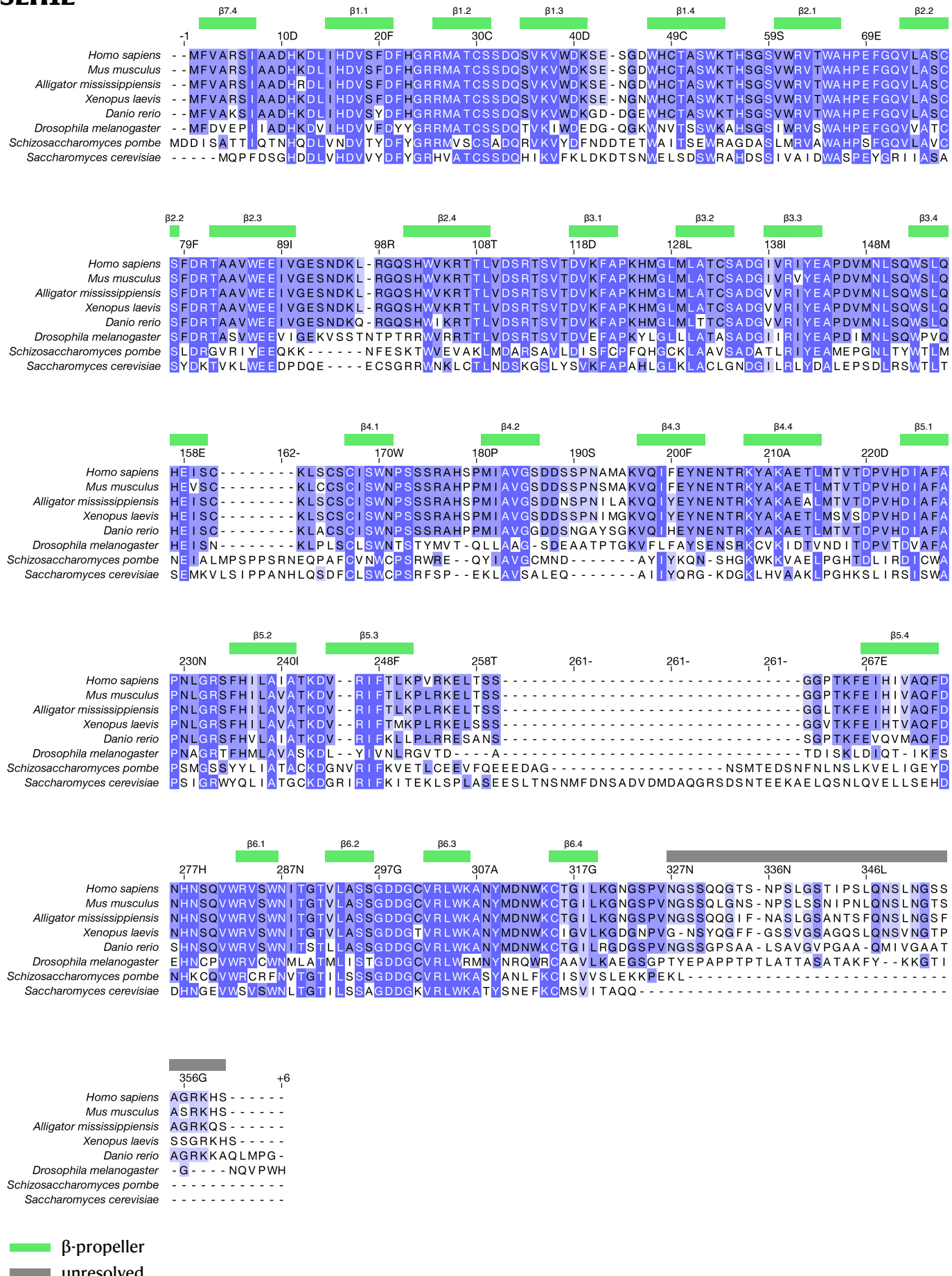
Supplementary Figure 7

WDR59



Supplementary Figure 8

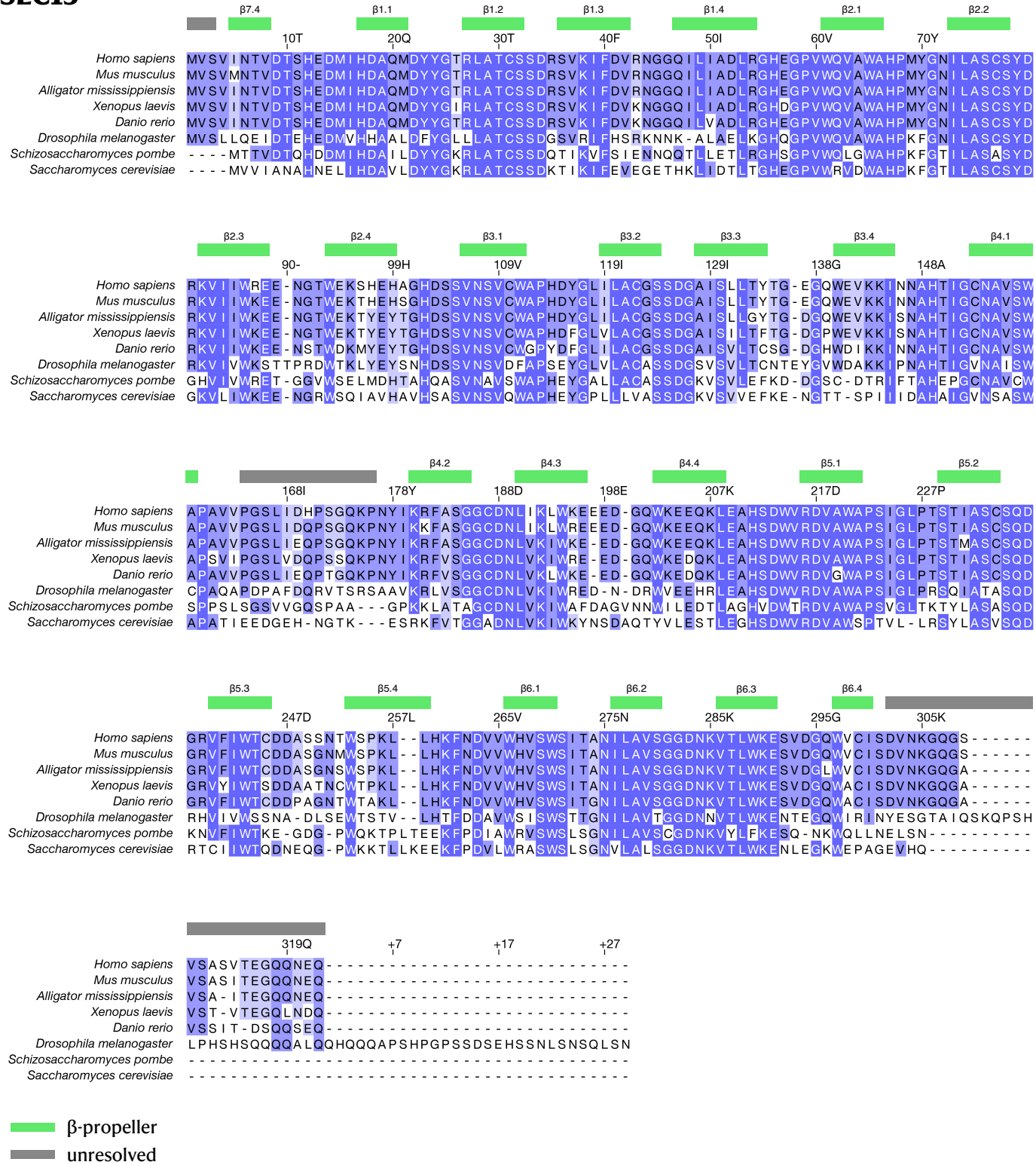
SEH1L



Supplementary Fig. 8 | Sequence alignment of SEH1L. Sequence alignment of SEH1L from various organisms. Residues are colored by percentage identity. Numbering refers to the human protein sequence. Secondary structure boundaries are indicated above the sequence alignment. Dark gray rectangles indicate regions unresolved in our cryo-EM structure.

Supplementary Figure 9

SEC13



Supplementary Fig. 9 | Sequence alignment of SEC13. Sequence alignment of SEC13 from various organisms. Residues are colored by percentage identity. Numbering refers to the human protein sequence. Secondary structure boundaries are indicated above the sequence alignment. Dark gray rectangles indicate regions unresolved in our cryo-EM structure.

Supplementary Table 1

Cryo-EM data collection, refinement and validation statistics

	GATOR2 global	GATOR2 local #1	GATOR2 local #2	GATOR2 local #3	GATOR2 local #4	GATOR2 local #5	GATOR2 composite
	#1 UMass	#2 MIT.nano	combined #1 and #2 C2-expanded	combined #1 and #2 C2-expanded	combined #1 and #2 C2-expanded	combined #1 and #2 C2-expanded	combined #1 and #2 composite of local maps
Data collection and processing							
Magnification (calibrated)	76,415	74,176					
Voltage (kV)	300	300					
Electron exposure (e ⁻ /Å ²)	44	47					
Exposure time (s)	2.4	4.0					
Defocus range (μm)	0.8 - 2.0	0.8 - 2.0					
Pixel size (Å)	0.530	0.546					
Symmetry imposed	C2	C2	C1	C1	C1	C1	pseudo C2
Initial particle images (no.)	913,619	6,324,254					
Final particle images (no.)	778,084	combined datasets	666,069	486,346	413,540	191,791	337,214
Map resolution (Å) FSC threshold = 0.143	3.66		3.53	3.37	3.38	3.84	4.45
Map resolution range (Å)	2.5 - 6.5						-
Refinement							
Model resolution (Å) FSC threshold = 0.5							3.48
Model composition							
Non-hydrogen atoms							51810
Protein residues							7314
Ligands							32 (Zn ²⁺)
B factors (Å ²)							
Protein							185.85
Ligand / ion							159.73
R.m.s. deviations							
Bond lengths (Å)							0.003
Bond angles (°)							0.434
Validation							
MolProbity score							1.21
Clashscore							4.34
EMRinger							2.21
Poor rotamers (%)							0.35
Ramachandran plot							
Favored (%)							98.12
Allowed (%)							1.88
Disallowed (%)							0.00
EMDB accession code	26519 additional map	26519 additional map	26519 additional map	26519 additional map	26519 additional map	26519 additional map	26519 main map
PDB accession code							7UHY

Supplementary Table 1 | Summary of cryo-EM data collection, 3D reconstruction, and model refinement.